LITERATURE REVIEW OF TSUNAMI SOURCES AFFECTING TSUNAMI HAZARD ALONG THE US EAST COAST

STEPHAN T. GRILLI, JEFFREY C. HARRIS AND TAYEBEH TAJALLI BAKHSH

DEPARTMENT OF OCEAN ENGINEERING, UNIVERSITY OF RHODE ISLAND
NARRAGANSETT, USA

RESEARCH REPORT NO. CACR-11-08
FEBRUARY 2011

Prepared as part of
NTHMP Award # NA10NWS4670010
National Weather Service Program Office
Project Dates: August 1, 2010 – July 31, 2013
Recipients: U. of Delaware (J.T. Kirby, PI); U. of Rhode Island (S.T. Grilli, co-PI)

CENTER FOR APPLIED COASTAL RESEARCH

Ocean Engineering Laboratory
University of Delaware
Newark, Delaware 19716

TABLE OF CONTENTS

1. BACKGROUND

The Uni ersit of Dela are and the Uni ersit of Rhode Island ha e been funded since 2010 b NOAA’s NTHMP program, to perform model simulations of tsunami generation, propagation and impact on the U.S. east coast, in order to establish tsunami inundation maps in regions of ele ated hazard or in areas deemed at higher risk. Such studies first require to identif , select, and parameterize, rele ant tsunami sources (both distant and local) in the Atlantic Ocean basin, hich go ern East coast tsunami hazard. This is particularl important for densel populated lo -l ing areas, hich ma be highl ulnerable to tsunami impact.

In the Pacific Ocean basin, tsunami hazard assessment, along the U.S. West coast, Alaska, and Ha aii, has long been studied on the basis of substantial historical records of relati el frequent tsunamis. While much fe er records of historical tsunamis e ist for the U.S. East coast, it is belie ed that about 10 percent of tsunami e ents that ha e affected the U.S. originated in the Atlantic basin (i.e., Atlantic, Gulf of Me ico, Puerto Rico, the lesser Antilles, and Virgin Islands; see Dunbar and Wea er, 2008). Not much is kno n, ho e er, about their related coastal hazard (not to mention their return periods).

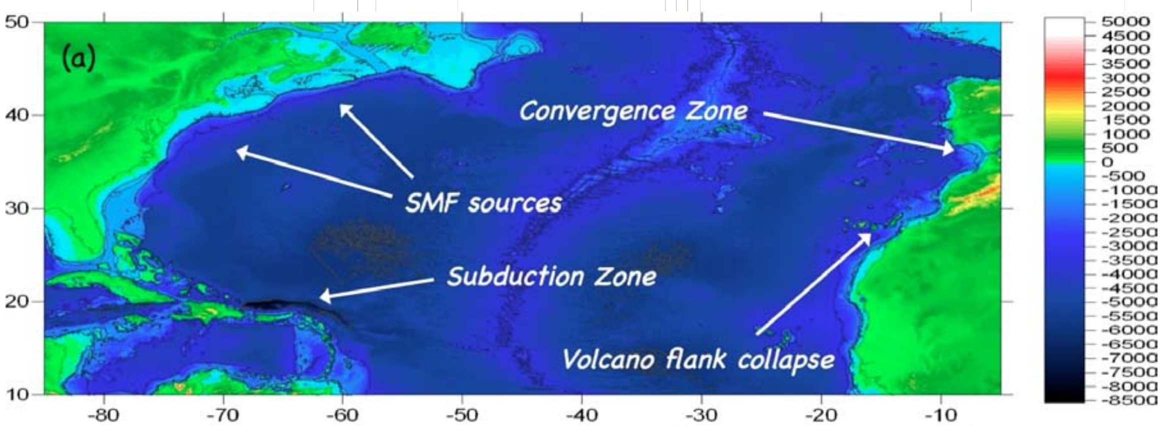

Fig. 1: Potential tsunami sources for U.S. east coast in the North Atlantic Ocean basin (ETOPO2’s t o second arc length ocean bath metr is sho n in the background).

Historical tsunami e ents in the Atlantic Ocean basin, that can affect the U.S. East coast, include (Fig. 1):

1. transoceanic co-seismic tsunamis, caused b earthquakes in the Azores-Gibraltar con ergence zone (e.g., Lisbon earthquake in 1755; Barkan et al., 2009);
2. transoceanic co-seismic tsunamis, caused b earthquakes along the Hispaniola-Puerto Rico-Lesser Antilles (a.k.a., Caribbean) subduction zone, in and around the Puerto Rico Trench (PRT) or near the Lee ard Islands (see, e.g., Grilli et al., 2008; 2010a);
3. a transoceanic landslide tsunami caused b a large mass failure e ent: the potential flank collapse of the Cumbre Vieja Volcano in the Canar Islands (see, e.g., Ward and Da , 2001; Grilli et al., 2006; Pérignon, 2006; Gisler, 2006; Lø holt et al., 2008; Abadie et al., 2009, 2011).

4. landslide tsunamis caused b Submarine Mass Failures (SMF), triggered along the East coast continental slope b moderate seismic acti it . Earlier field and modeling ork (tenBrink et al., 2007, 2008, 2009a; Grilli et al., 2006, 2009), indeed, indicates that the most significant tsunami hazard for the U.S. East coast ma result from such near-field landslide tsunami sources, hich although less energetic than large co-seismic tsunamis, could occur at a short distance from shore (in terms of tsunami propagation time) and hence cause significant runup on small sections of the coast hile offering little arning time, thus posing significant hazard to local, lo -l ing, coastal communities.

2. LITERATURE REVIEW OF RELEVANT TSUNAMI [illegible]RCES

In this report, e focus less on specific e ents and more [illegible]nformation about [illegible]tial sources required to setup numerical models of tsunami g[illegible]ation and propagat[illegible] ith hich to stud hich tsunami sources (and their paramet[illegible]ma go ern tsunam[illegible]zard (in terms of runup and inundation) along the U.S. East co[illegible]In a later phase of [illegible] ork e ill quantif this hazard through numerical simulati[illegible]in a series of neste[illegible]odel grids, for arious coastal communities deemed important [illegible]entified to be at hig[illegible]risk, in the form of detailed inundation maps.

For information on specific historical e ents and a[illegible]ef histor of tsunam[illegible]n the Caribbean sea, see, e.g., Lockridge et al. (2002), hich i[illegible]des a catalog of 40 [illegible]erent tsunami or tsunami-like a es that ha e struck the U[illegible]East coast since 1[illegible] and Lander et al (2002) ho catalogued 91 reports of a e[illegible]at ma ha e been [illegible]amis since 1498. Recent studies commissioned b the Nuclea[illegible]egulator Commissi[illegible] ha e also been conducted b the USGS, regarding potential tsu[illegible]mi sources affecting [illegible] U.S. East Coast (ten Brink, 2007, 2008). Additionall , the N[illegible]A Forecast Source [illegible]abase (http://nctr.pmel.noaa.go /propagation-database-access.ht[illegible]) pro ides a distan[illegible]ource catalog, for the purpose of inundation modeling, rec[illegible]nizing that the depi[illegible]on of potential tsunami sources ill e ol e and change ith [illegible]e and that, due to i[illegible]lo er percei ed risk, the Atlantic ocean is not er ell co ere[illegible]

In the follo ing, e detail a ailable data for [illegible]ach t pe of tsunami[illegible]ources go erning the U.S. East coast tsunami hazard (Fig. 1).

2.1 Submarine Mass Failures

Submarine Mass Failures (SMFs), hen tsunamigenic, i[illegible]ld potential near-field [illegible]unamis sources that ma go ern tsunami hazard along the entire [illegible].S. East coast. Althoug[illegible] onl a fe historical landslide tsunamis ha e been clearl ident[illegible]fied in the region, ten Brink et al. (2007) and T ichell et al. (2009) report that one third [illegible]f the Ne England co[illegible]tinental slope and rise is co ered ith landslide scars and dep[illegible]osits. Based on their detailed description of field data (see, e.g., Tables 2-1, 2-2 and F[illegible]gs. 2-4, 2-7, 2-8 in ten Brink et al., 2007), and arious statistics performed on these, e [illegible]find for the largest SM[illegible] scar off of the U.S. East coast, a 15,241 km^2 area, 291 km length, 151 km idth, 3,263 m a erage depth, ith a 4,735 m toe depth and a 1,260 m scarp height, ielding a er large olume (for 34 listed slides in their Table 2-2, olume aries bet een 0.08 and 179 km^3). Furthermore, the same ork sho s that roughl 50% of the area affected b landslides, and 7 of the 14 landslides in the list that co er areas e ceeding 2,000 km^2 are located offshore of Georges Bank and southern Ne England (a region that co ers appro imatel one third of the length of the stud area). Another 24% of the area affected b landslides occurs as t o large ones in the Carolina Trough. The remaining 25% of all landslides are spread along the remaining half of the length of the stud area. SMFs ith olumes abo e 100 km^3 (of there are 4 isted in able 2-2) can generate ru f more than t o meters on coats (e.g., Grilli t al., 2009). The actual tude of landslide-generated t his, ho e er is er te specific and depends on detailed geometr , location, olume, as ell as on the mode of rupture (Gril Watts, 1999, 2005; Watts et 005; Enet and Grilli, 007; ten Brink et al., 2009a st et al., 2009). Most of thes ameters are poorl kn n or unkno n for obser andslide scars.

Hence, for m otential SMFs, both the landslide e ents themsel and their tsunamigenic potent are a priori unkno n. Additionall , landslide ering b seismic acti it is n nl a comple phenomenon, but also one that de s on the magnitude of the sei ground acceleration e pected at some distance o re in the potential slide area (a gi en return period), hich is poorl kno n as o er the Atlantic ocean (in pa e to the paucit of obser ed earthquakes). As a par guidance, for the largest earth e e er obser ed along the Ne England margin, ich had a magnitude 7.0 suffic to trigger a significant SMF (hich it did in the 29 Grand Bank SMF and tsu , discussed belo), ten Brink et al. (2009a) esti e that the return period is bet 600 and 3,000 ears.

As a result o e lack of data and uncertainties listed abo e, a c rehensi e anal sis of SMF tsu mi hazard along the U.S. East coast is being con ted in this project, as a separate sk, based on Monte Carlo (MC) simulations of slope abilit and tsunami generation/r up, similar to the approach detailed in Grilli et al. (2 9). Such a MC anal sis ill pr ide statistical distributions of potential tsunamigen SMFs and their parameters, in t region of interest. Once alidated using field data (as as done b Grilli et al., 2009 fo e region from Ne Jerse to Cape Cod), such dist utions ill allo designing a se s of rele ant SMF sources, hich ill be used to antif East coast landslide tsu mi hazard b performing numerical simulations of tsunami propagation and coa l impact. In ie of this upcoming ork, e ill lim the present discussion of SMF t nami hazard to t o ell-kno n historical SMF cas , for hich landslide tsunamis re either generated, or strongl suspected to ha e be generated, along the East coast:

1. The first, and nl historical SMF tsunami definitel kno n to ha e mpacted the North Ameri an coastline, causing 28 fatalities, occurred on No ember 18th, 1929, as a res lt of a submarine landslide caused near the Grand Ba ks b a large earthquake th M_w = 7.2 moment magnitude (to date this still presents the largest earth uake e er recorded in the North American coastal r gions of the Atlantic bas). The large slope failure as triggered at the outh of the Laurentian C annel (Bent, 1994; 1995) on the south coast of Ne oundland, at 44.691°N–56 006°W (Fig. 2), 18 km from the 2 km deep upper continental slope (Fine et al., 2005). The landslide transformed into a turbidit current that flo ed o er 100 km along the Atlantic floor, at speeds of 60-100 km/h, displacing about 200 km^3 of material. Fine et al. (2005) used a iscous shallo ater model to simulate this e ent, treating the slide as a iscous, incompressible fluid la er. The estimated ma imum tsunami a e amplitude as 3-8 m and the ma imum runup

obser ed in Ne foundland as 13 m. While [redacted]region affected b such a landslide-generated tsunami as much smaller tha[redacted]at from a t pical co-seismic tsunami, such large runups posed a significant loc[redacted]hazard, as confirmed b the large number of fatalities.

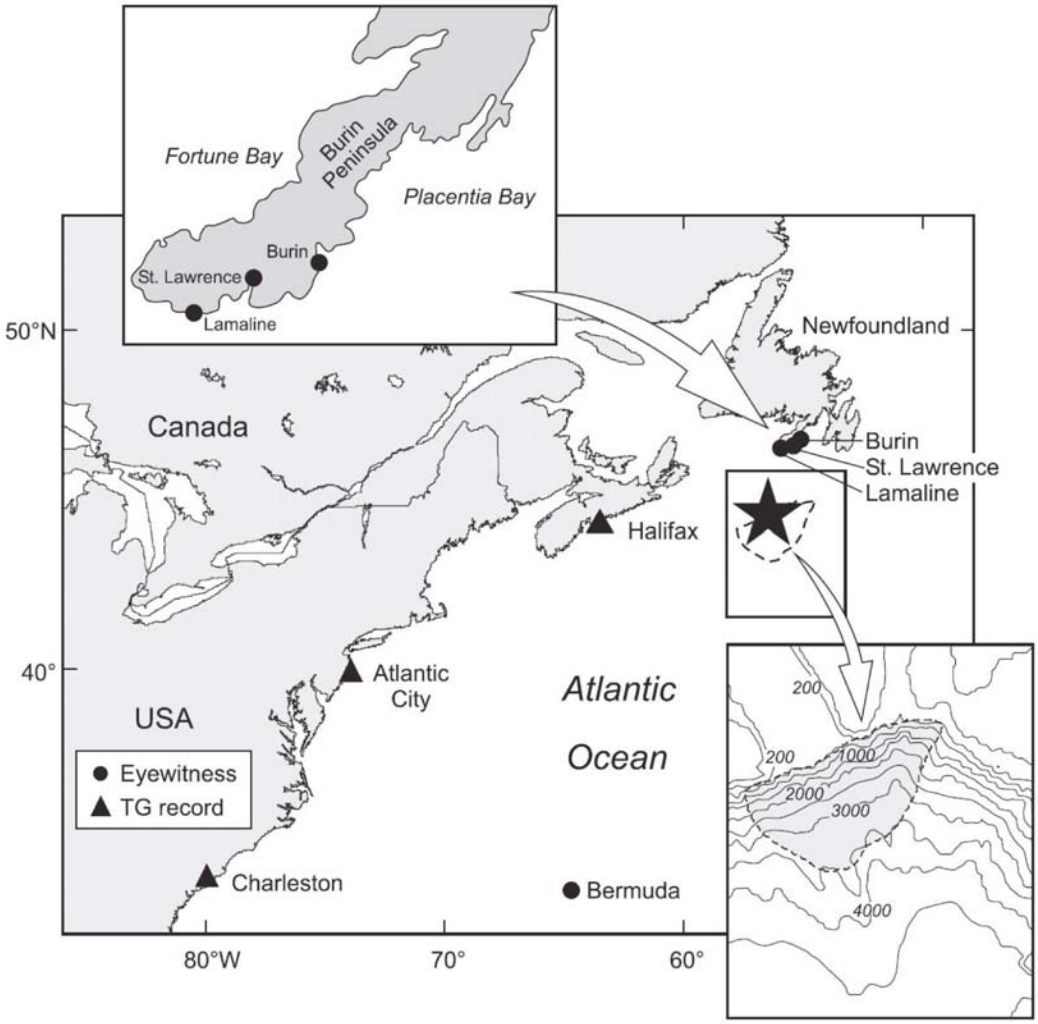

Fig. 2: Location of 1929 Grand Banks SMF, hich created a tsunami, noting locations here there ere e e itness or tidal gauge records of the e ent. The star denotes the earthquake epicenter, and the shaded region (lo er right inset) denotes the area of the slide. From Fine et al. (2005).

2. The second, and most notable landslide comple along the U.S. East coast is kno n as the Currituck landslide, about 100 km off the coast of Virginia and North Carolina (e.g., Fig. 2-9 in ten Brink, 2007). This translational slide is belie ed to ha e occurred bet een 22,500 and 43,300 ears ago and as likel a single e ent caused b an earthquake (Prior et al., 1986). The debris of the slide itself reached as far as 220 km from the shelf edge, and 190 km from the toe of the source area. The do n-slope length as about 30 km, the idth about 20 km, and the initial thickness as about 250 m (ten Brink et al., 2007, 2008). Volume estimates ar for this e ent, but the olumes, hich ere used b ten Brink et al. (2007) for performing simulations of tsunami hazard along the East coast for the

lea Regulator Commission, 8 to 165 km^3. Preliminar mulatio umb r of Currituck scenarios earshore a e heights of 5- m off o Je se Coast.

3. e tsu ami generated b this SM s modeled b Geist et al. (20 9), usin pers e long a e model CO AVE. Based on Locat e al.'s (2 bilit anal sis, the chose to si e one of three different lands lide olu her n e ent of 108 km^3, 57 k r a composite of the t o (1 65 km^3). h o the three slide scenarios, considered different slide durations tom friction coefficients. The und a large ariation in ma imum r oadside of the Currituck landsli rom 1.20 m to 8.80 m. The found tha ost critical parameter for tsunam eration as the landslide olume.

For s arine landslides, pre ious ork sho n that the tsunami generation so can b appro imated to a large degre using simple semi-empirical equa appro ating results of numerical mode mulations, based on geometric properti f the la lide (such as length, idth, thic ss, olume, and the slope incline), the k densit f the material, and some simple rod namic and friction coefficients. Th s comp tionall much faster than using a parate Euler or Na ier-Stokes simulati o mode andslide ph sics. This approa has been used to de elop semi-empi l lands e tsunami sources based on full nlinear 2D and 3D full nonlinear pote al flo ulations of idealized slide or slu cases (Grilli and Watts, 1999, 2001, 2 5; Grilli al., 2002, 2010b; Enet and Grilli, 03, 2005), and has been successfull ap ed to pe rm tsunami case studies (e.g., Wa et al., 2003, 2005; Da s et al., 2005; Ta in et al., 08). An earl ersion of this as scribed b Watts et al. (2005). See Appe i A for updated TOPICS implementation f SMF sources.

2.2 C -seismic tsunamis

The c -seismic bottom displacement res lting from large magnitude earthquakes .e., greate than M = 6.5 or so), occurring a small depth belo the seafloor, ma gen rate signif cant tsunamis, depending on a ari t of geological, geographical, and earthq ake param eters. Based on ell-kno n geolog and tectonics, co-seismic tsunamis gene ted b la ge earthquakes in the North Atla tic ould either originate in the Carib ean subdu tion zone or the Azores-Gibraltar con ergence zone (Fig. 1). Each of these has uniqu e characteristics.

2.2.1 Review of literature on Caribbean subduction zone

The Caribbean plate is one of the smallest plates in the orld (Figs. 3, 4). It ha s an appro imatel rectangular shape and e tends from Central America to the L esser Antilles, and from South Cuba to the South America. The plate pushes its a east ard (at 20-25 mm a ear) against the much larger (subducting) North American and South American plates (see, Zahibo et al., 2001, and their Fig. 1 for the geod namic conte t of faults in the area; ten Brink, 2007; Jansma, 2008).

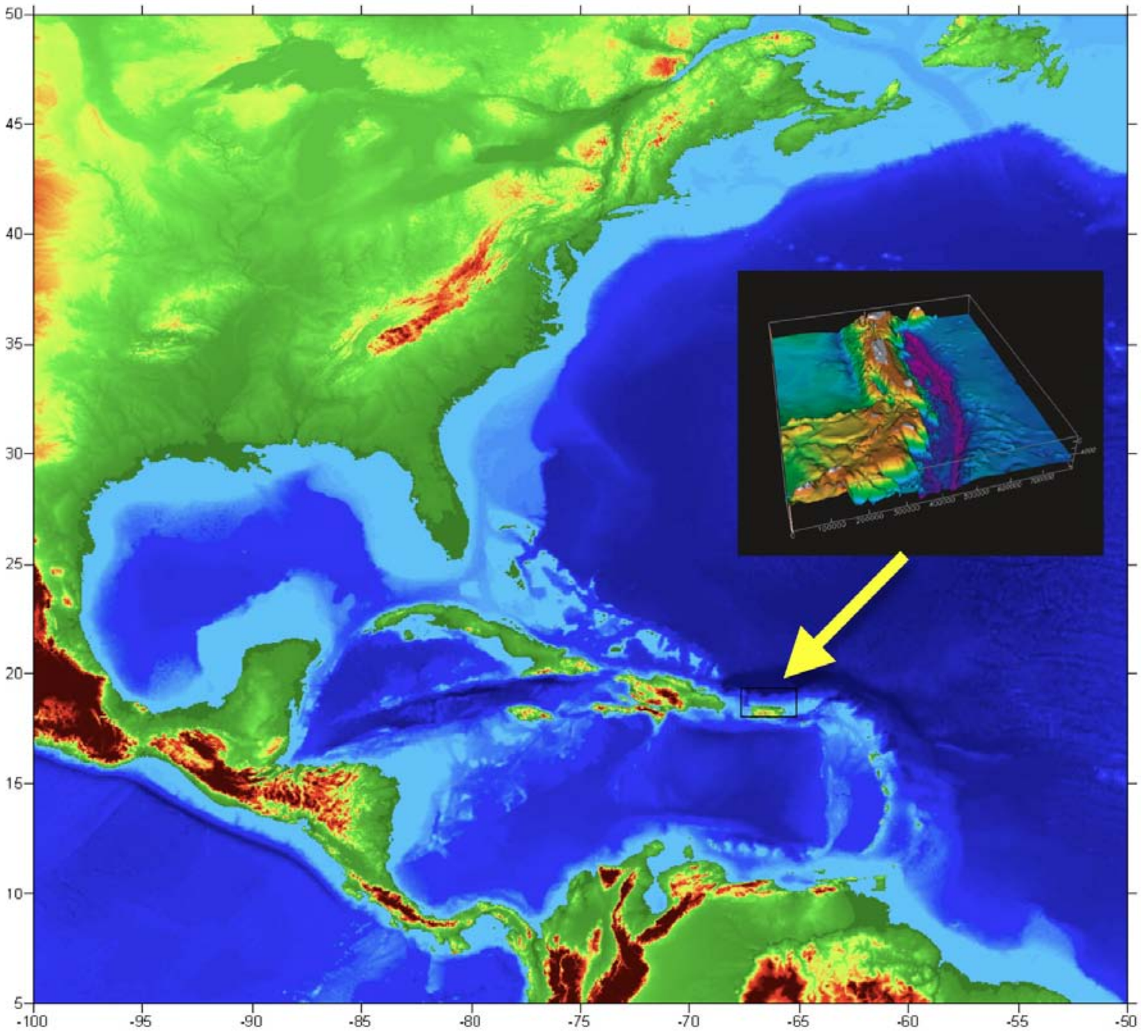

Fig. 3: ETOPO-2 bathymetry (2’ accuracy) for the NW Atlantic Ocean basin (axes are in degrees of N Lat. and W Long.). The island of Puerto Rico is marked by a black rectangular box, approximately 204 by 126 km. The sub-figure shows topography and bathymetry in and around Puerto Rico; the 770 km long, 50 km wide, and 7 km deep Puerto Rico Trench (PRT; pink color) is to the north of the island (USGS, 2001).

Its motion ith respect to the North American plate causes olcanoes and earthquakes in the region (Zahibo et al., 2003b). The Puerto Rican Trench (PRT; Figs. 3, 4) is at the boundar bet een these t o plates. Figure 3 (sub-figure) sho s the topograph and bath metr around the deep PRT, north of the island. The trench is appro imatel 770 km long and 50 km ide, ith a depth reaching o er 7,000 m (up to 8,340 m at one location). The northeastern portion of the Caribbean Plate is thus the general tectonic setting for Puerto Rico and the PRT, ith the island l ing ithin the East-West trending plate boundar zone (Fig. 4), bet een the WSW mo ing North American Plate (to the North and right on sub-figure 3) and the ENE mo ing Caribbean Plate (left on the sub-figure; Mercado and McCann, 1998).

More specifica ll , the North American e subd nder the Caribbean plate, at a rate that has been estimated from about 2 n per (DeMets, 1993) to 37 mm per ear (S kes *et al.* 1982). As in other rec udies the PRT area (Zahibo and Pelino sk , 2001; USGS, 2001; ten Brink and , 2004 Brink, 2005, 2007; Jansma, 2008; Grilli et al., 2010a), e assume in follo anal ses that there is a predominantl (lateral) strike-slip motion of th aribbea te at 20 mm per ear ith respect to the North American Plate, in the E irectio a 10-20 degree angle ith respect to the trench a is.

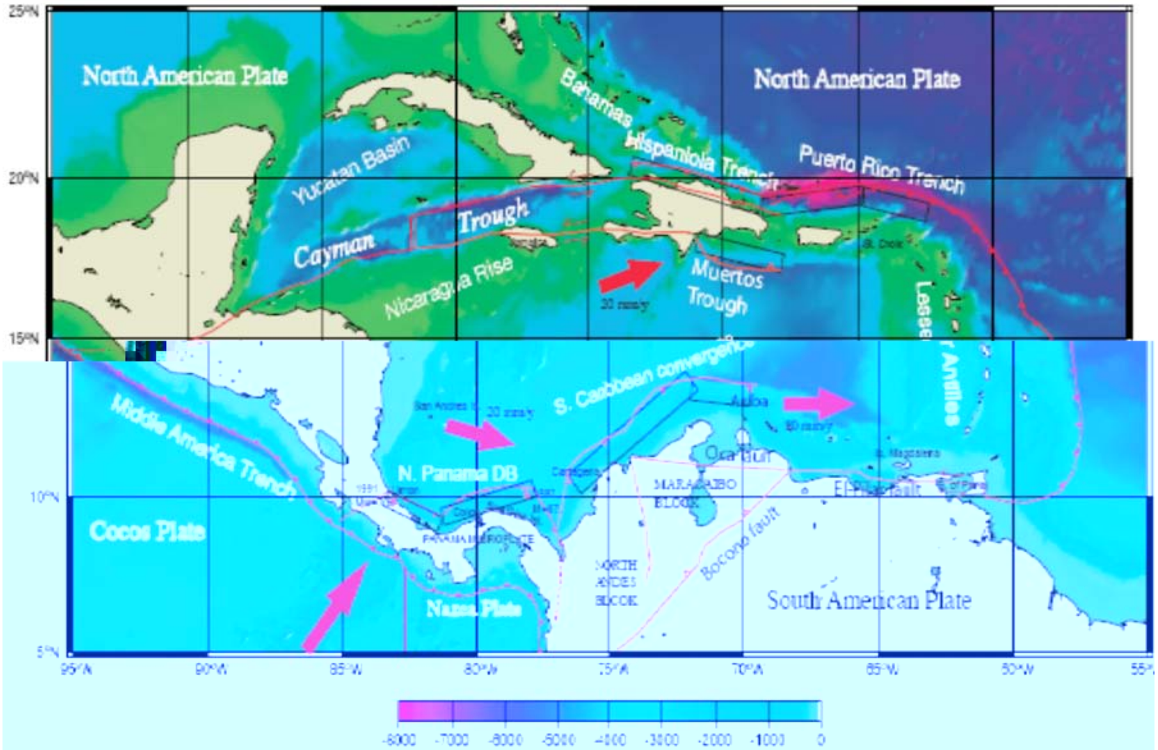

Fig. 4: Boundaries of Caribbean plate with various relev nt islands a convergence rates, as well as faults and trenches (from t n Brink, 200).

Historical anal ses of tsunami e ents n the area o erl ing the Caribbean plate (including the Caribbean Sea) ha e catalogued 27 likel andidates (Lander et al., 2002; O'Loughlin et al., 2003; Caribbean Tsunami Hazard, 2006). While some of these candidates ha e been caused b olcanic eruptions, ost ha e been generated b under ater earthquakes. One of the most deadl e ents among those, the 1918 Puerto Rico tsunami, as generated b a 7.3 magnitude earthquake in the Mona Passage (15 km off the north est coast of Puerto Rico, appro imatel 24.2 km est of Punta Higuero) and caused major damage on the West Coast of Puerto Rico (up to 6 m runup and 116 fatalities; Mercado et al., 1998). Mercado and McCann (1998) simulated this e ent using a linear model for the far-field and a nonlinear model for runup. The oldest recorded tsunami near Puerto Rico occurred in 1867, and as caused b a 7.5 magnitude earthquake in the Anegada Passage (bet een St. Croi and St. Thomas, US Virgin Islands). The source length as about 10 km, the ertical displacement of the sea floor as less than 10 m, and the strike of the fault as appro imatel E-W. This e ent as modeled b Zahibo et al. (2003a) ith the nonlinear shallo ater equations. The used different orientations for the tsunami source and in estigated the directi it of the a e and distribution of a e height.

While man faults are acti e in and around the Caribbean, due to its location and predominantl E-W orientation, the PRT ould be most likel to cause tsunamis that could reach the U.S. East Coast (see, e.g., Grilli et al., 2010a). As a result of the large component of relati e strike-slip motion of the Caribbean plate against the North American plate, frequent small to moderate earthquakes occur in the PRT region (see, Zahibo et al., 2003, their Fig. 1, and ten Brink, 2005, for historical maps of seismicit in the larger Caribbean Sea area), for hich ten Brink (2005) mapped the depth and intensit (for $M > 2.5$); earthquake locations are clearl aligned ith the boundar of the subducting plates. B contrast, the same anal sis onl identifies 6 large historical e ents of magnitude 7 or greater (a t pical threshold for potentiall large tsunami-genesis; Table 1), for the past 220 ears in or near the PRT. Among these, t o e ents occurred ith (estimated) magnitude greater than 8, and four reportedl generated a tsunami, ith three causing a 5-7 m runup on Puerto Rico (cases 3-5; USGS, 2001; Zahibo et al., 2001, 2003; Lander et al., 2002). For completeness, it as also reported b Da icki (2005) that t el e earthquakes of magnitude 7 or greater occurred near Puerto Rico in the past 500 ., but no additional tsunami records, other than those presented in Table 1, ere gi en.

Earthquake location	Date	Magnitude	Tsunami	Casualties	Runup (m)
1. Hispaniola	1953	6.9			
2. Mona Passage	1946	7.5	Yes	40	
3. Hispaniola	1946	8.1	Yes	1,800	5
4. Mona Passage	1918	7.3	Yes	91–116	6
5. Anegada Trough	1867	7.5	Yes	?	7
6. Puerto Rico Trench	1787	8.1			

Table 1 : Largest historical seismic e ents around Puerto Rico (USGS, 2001).

The catastrophic 7.0 magnitude (shallo) earthquake that hit Haiti (on the island of Hispaniola just West of Puerto Rico; Fig. 4) on Jan. 12th, 2010, hea il damaging Port-au-Prince and killing o er 217,000 people in the process, recentl reminded us of this potential for large earthquakes in the area. While this earthquake as mostl land-based and onl generated a small tsunami, a large ocean-based earthquake in the PRT could generate a significant tsunami that might ha e catastrophic effects in the near-field on the lo er l ing coastal areas of the Puerto Rico North Shore (e.g., San Juan), as ell as induce significant far-field effects on distant shores, including the US East Coast (see, e.g., Grilli et al., 2010a). Mercado et al. are conducting NTHMP funded tsunami simulation ork to create tsunami inundation maps along the Puerto Rico shore. Hence, here, e focus on future e ents in the PRT (and nearb faults) hose far-field impact could affect or go ern the East coast tsunami hazard. Because of the lack of large earthquakes in the PRT in the past 200 ears (Table 1) a large and potentiall tsunami e ke should b pected the nea future. In te and Lian's ( ) r ur e of the T unco ed e ide e of curre is it and inte str ld-up in the duction one nea he PRT, s the "impend oc e of a poten l large rthquake n the trenc d the urgenc esti tsunami haz in the re on and in e far-field r t.

A ordi here has bee ubstantia ecent re arch into d ng able earthqua scen o perform si ations of sunami g neration and im n the resulting ar-fi d far-field ts mi hazar (e.g., Knight, 2006). o lli et al. (201 e a belo the r nale for e eloping such scenar i lude both est ted e uake paramet and retur period.

Althoug r gorous anal s of earthquake and ts nami return rio ld be difficult o per m due to the p cit of o ser ation of large s mic and tsunami n the i n (onl one hi rical e en , case 6 in Table 1, is s cifi ed in the PRT it ap ar from data in able 1 tha there e 3 large ts mig ic ents affecting Puert ic during an 80 ear period and 5 large earthquakes rin 16 ear period i the Pu to Rico area, t of those ith magnitude greater t n 8. nc , as a first app o ima n, one can ass ate a magnitude 7.5-8.1 seismic ent th area around uerto o ith a 30 to 8 ear return period. Similarl , Da ki's 00) data ould ld an erage 42 ear ret n period, for e ents of magnitude r gr ter, hich is consi ent i the latter data. L ger period e ents ha e not been o er e but based on estim ated pl es' subduction ra and appro imate ma imum lengt and dth of the PRT are that uld mo e during future large scale e ent, one coul tr d estimate the magnitude f e treme seismi e ents in the trench, as a functi of heir return period. This is d scussed belo .

To prepa e for the impact o the U.S. East coast from future ma or tsu amis in the Caribbean regi n, Knight (2006) e eloped a first-order estimate of he m st e treme earthquake that could occur in th PRT, and assessed the resulting poten al tsunami hazard (mostl for the Caribbean slands and lo er East coast). Although Knight's as not an e tensi e anal sis, it sho ed that onl the largest earthquakes f om th Caribbean subduction zon should be of concern for the U.S. East coast, and the foc s of future ork should be on sources originating in the PRT. More specificall , i his ork, Knight assumed a simple homogenous source model (i.e., ithout considering effec s of shores, small islands and archipelagos), co ering a 600 km b 150 km area of the Puerto Rico trench (i.e., nearl the full E-W e tension of the PRT b three times its actual idth), ith a fault plane orientation based on the PRT geolog (angles are gi en in a follo ing section). This e treme source corresponded to a magnitude 9.1 earthquake, hich using Okada's (1985) method ields an a erage slip of $\overline{\Delta}$ = 11.9 m (and ma imum slip of Δ = 19 m; see details of our slightl modified ersion of the method in Appendi A). Based on the estimated 20 mm per ear subduction rate in the region, this a erage slip ould ield a long return period earthquake of 600 ear or so. No , if the t o largest historical e ents of magnitude 8.1 listed in Table 1 had affected the same (entire) area of the PRT, one could estimate their return period b prorating a erage slip to the released energ , as compared to the 9.1 e ent (note, under Okada's (1985) method assumptions, total energ released b an earthquake is proportional the as med rfac area and a erage slip; see appen i A for details). This can b done u ng l ks d Kanamori's (1979) relationshi bet een energ M_o [J] release b an e thqu e a its moment magnitude defined as: M_w = log M_o/1.5 – 10.7 (here 51 = lo 32.3 h h for a er significant M =8.81 e ent ields an a erage slip: $\bar{\Delta}_{8}$ = $\bar{\Delta}_{9.1}$ 2.3 1-8.1) 0.37 m. Based on the estimated subduction rate in the PRT, thi ould l r esen a 20 ear or so return e ent, hile historical data points to a lon er 30-8 ea turn eriod. This implies, as could be e pected, that in such smaller bu still sig ifica e e s onl a fraction of the length of the PRT as likel mobilized b he earth uake or i tance, for the same M_w = 8.1 e ent, due to the proportionalit f releas d en g t slip and surface area, reducing the affected length of PRT to 300 km ou l incr se a erage slip to 0.74 m and the estimated return period to 40 ears o so. Not , this ould also ha e the effect of proportionall increasing the initial tsuna i source and rther concentrating its effects on lands and islands closest to the earthqua e area, round he PR T. Ho e er, since no or fe obser ations ere made for these hist rical e nts, it is nea l impossible to further constrain the tsunami source based on h drod nami obse ations (as, e.g., as successfull done for the idel obser ed 2004 Ind an Oc an Ts nami; see, e.g., Grilli et al., 2007; Ioualalen et al., 2007).

Grilli et al. (2006, 2010a) performed numerical simulations of near- and far-field tsunami impact on the basis of Knight's e treme "600 ear" 9.1 magnitude source (Fig. 5). Additionall , as it as desirable to estimate the likel ma imum e ent that could occur in the PRT in the near future, Grilli et al. (2010a) de eloped a 200+ ear return period source, affecting the entire area (600 150 km) of the PRT, based on accumulated potential slip in the trench since the last kno n e ent that significantl affected it in 1787, i.e., 223 ears ago. This represents a $\bar{\Delta}$ = 4.46 m a erage slip and the resulting source for this e ent has a 8.7 magnitude and ma imum slip $\Delta_{8.7}$ = 4.72 m.

Finall , for completeness, other ork focused on the Caribbean Sea and Lesser Antilles, S and SE of Puerto Rico, here local earthquakes and olcanic eruption could (and ha e) caused regional tsunamis. These ho e er, ould be too small and/or some hat blocked b Puerto Rico, to ha e a significant impact on the U.S. East Coast. Thus, Zahibo and Pelino sk (2001) e aluated the tsunami risk in the Caribbean Sea area, hich includes both earthquakes and olcanoes. The find that co-seismic tsunamis ould be likel larger in the region than landslide or olcanic tsunamis. Zahibo et al. (2003b), using a model based on the nonlinear shallo ater equation, simulated potential tsunamis in the Caribbean Sea and their impact on arious coasts. Based on historical data, the mentioned the Caribbean crossing time ould be about 3.2 hrs for lateral transfer and 1.2 hrs for meridional crossing. Nikolkina et al. (2010) anal zed historical tsunami data for the region around Guadeloupe, and found that the French West Indies subduction zone has the potential for tsunamigenic earthquakes of up to M_w = 8.3. The also reported reliable and alidated data regarding historical e ents in the Caribbean Sea, indicating that the return period for tsunamis in the Caribbean is about 3 ears (although man are onl local e ents, and not all of the historical records are definiti e).

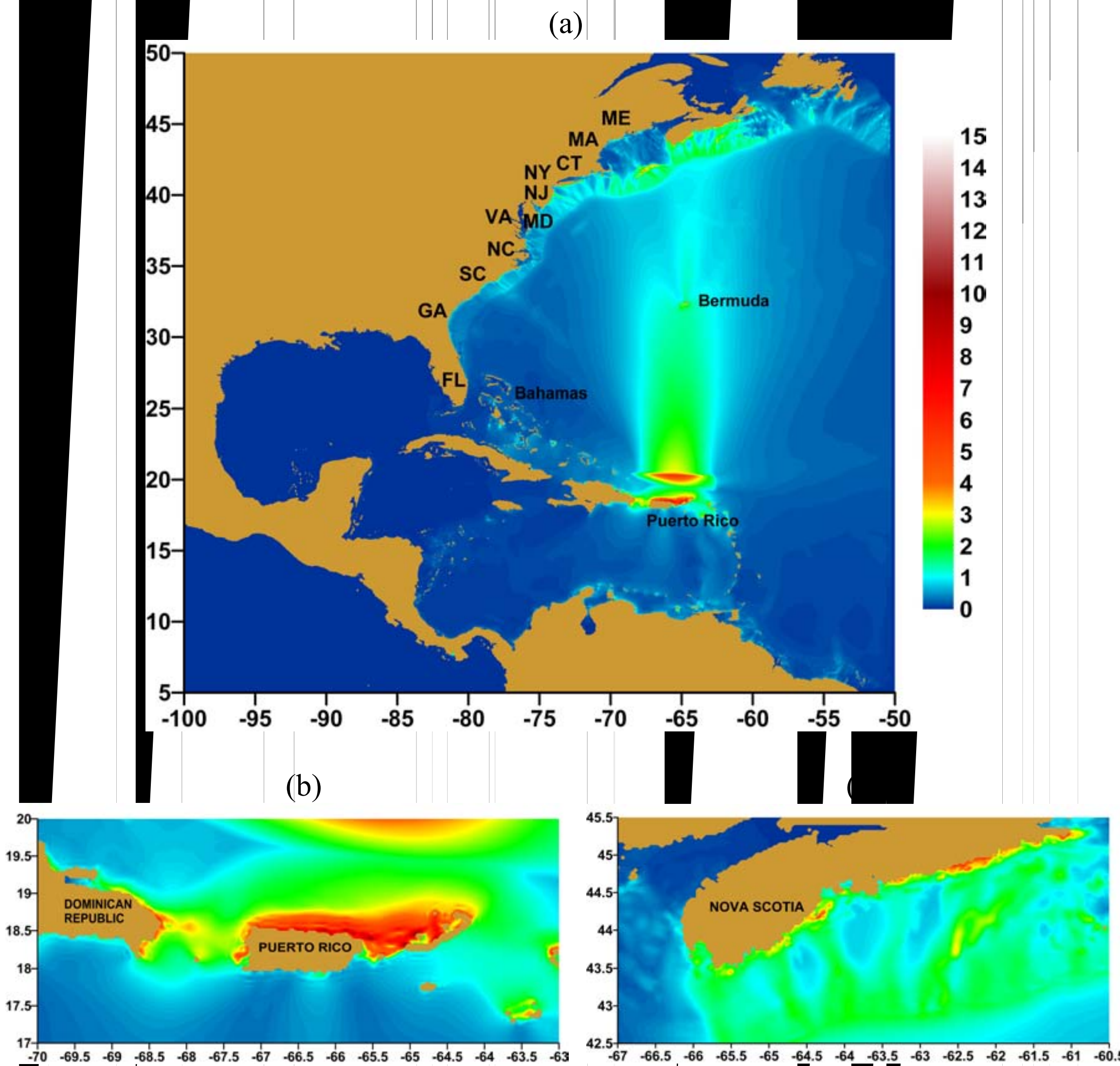

F g. 5: Grilli et al.'s (2010a) FUNWAVE simulations o er a 2' 2' grid for a 9.1 c -seismic tsunami source in PRT (a es are in degrees of N Lat. and W Long.): (a-c) Ma imum surf ce e ations (color scale in meter) at an time during computations. Zoom near and around (b): Puerto R co; (c): No a Scotia.

Based on the abo e, for simulating the far field effect on the U.S. east coast of large co-seismic tsunamis initiated in the PRT, e propose to use Grilli et al.'s (2010a) e treme (600 ear) M_w = 9.1 source, affecting the entire PRT 600 150 km area. Fig. 5 sho s Grilli et al.'s (2010a) FUNWAVE results for the ma imum tsunami ele ation caused b this source, in both the near- and far-field, in a coarse 2' 2' Atlantic basin grid, using ETOPO-2 ocean bath metr merged ith the NGDC 3" Coastal Relief Model (Di ins and Metzger, 2008) belo 19 deg. N, North of Puerto Rico. Fig. 6 sho s an e ample of coastal impact computed for this e ent, in a finer 15" 15" regional nested grid, along the U.S. East coast from Ne Jerse to Cape Cod (MA). Additionall , e ill use a series of 200 ear M_w = 8.7 sources, the first one being similar to Grilli et al.'s (2010a) and others onl affecting a reduced length of the PRT of 300-400 km, ith the source epicenter mo ed among a fe locations, from E-W (e.g., 4).

Quantitie[redacted]	[redacted]source	8.7 source
Epicenter [redacted]	[redacted]° N 66° W	19.5° N 66° W
Strike (de[redacted]	[redacted]	92
Dip (degr[redacted]	[redacted]	15
Rake (deg[redacted]	[redacted]	50
Ma imum[redacted](m)	[redacted]	4.72
Fault plan[redacted]th (km)	[redacted]	40
Length (k[redacted]	[redacted]	600

Table 2: Ok[redacted] parameters for 9.[redacted] 8.7 sources for Grilli et al.'s (2010a) FUNWAVE simulations.

(a)

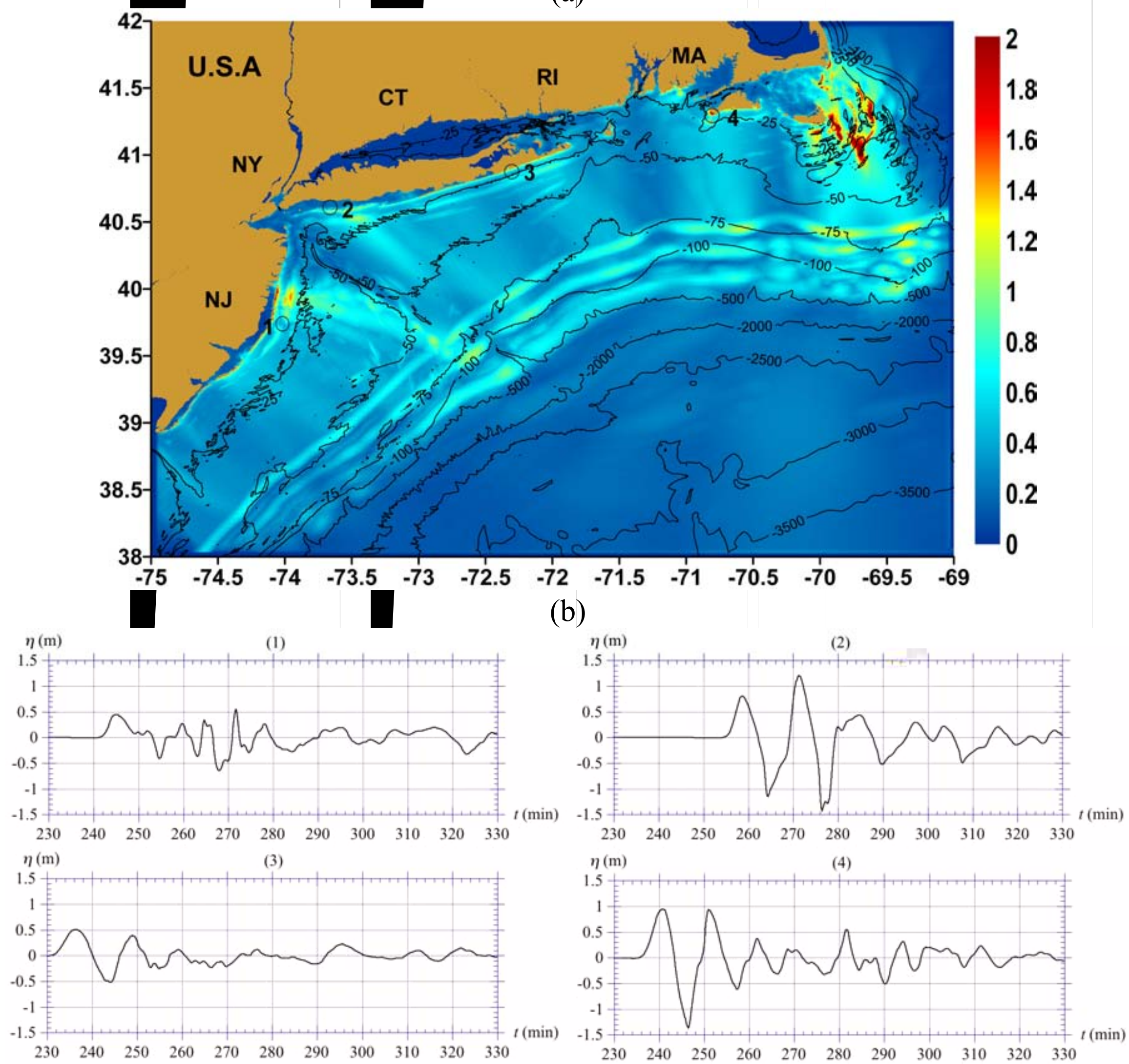

Fig. 6: Same case as Fig. 5. (a) Ma imum tsunami ele ation for the Ne Jerse , Long Island, Rhode Island and Cape Cod coastal areas, in a nested 15" regional grid (initialized ith Fig. 5 results; color scale in meter; a es are in degrees of N Lat. and W Long.); (b) time series of tsunami arri al at locations 1-4 (numerical gages) marked as s mbols (o) in Fig. (a), ith depth 14.4, 3.2, 18.1 and 14.8 m, respecti el ; times correspond to the start of the tsunami e ent in the PRT.

Okada's parameters used for generating these sources with TOPICS are given in Table 2. Note, these two sources are consistent with ten Brink and Lin's work (2004), who stated that the worst-case scenario for an earthquake rupture along the PRT is a single 675 km long rupture, between 68°W and 62°W. As an example, for a 10 m average slip and shear modulus $\mu = 3 \times 10^{10}$ Pa, the rupture area 675 by 102 km, the moment is $M_w = 8.9$, which is in the proposed range for our work.

2.2.2 NOAA Forecast Source Database for Caribbean subduction zone

The NOAA Center for Tsunami Research (NCTR) has produced a series of model runs corresponding to various faults around the world (Gica et al., 2008). For the Caribbean subduction zone, this consists in a series of 214 different sources, with 1 m average slip, a fault length of 100 km, width of 50 km, and generating an energy corresponding to a M_w = 7.5 moment magnitude earthquake. Based on available data about various faults, reasonable estimates of the epicenter longitude and latitude, strike angle, dip angle, and depth of the unit sources are provided. Based on NOAA's unit source simulations, maps of maximum tsunami elevations can be produced, such as Fig. 7 for one of these unit sources. We see that while overall far-field impact depicted in Fig. 7 follows a pattern similar to that in Fig. 5a, the maximum elevation is much reduced (by about a factor 100 in the U.S. upper East coast), consistent with the much reduced energy in a 7.5 source, as compared to a 9.1 source (factor of 110 based on Kanamori's relationship). Note, the concentration of wave energy in Fig. 7 off of South Carolina, which is also present in a large number of NOAA's unit source simulations and is likely caused by wave focusing on Blake ridge.

While the work of Gica et al. (2008) was primarily aimed at producing tsunami elevation to be used in the Caribbean basin for the Short-term Inundation Forecast for Tsunamis (SIFT) system (an operational tool for rapid forecasts of tsunami impact), rather than creating a worse case scenario in the far field, such results can be used in the present work to better understand both the types of impacts from tsunamigenic earthquakes in the area, as well as providing a rough estimate of expected FUNWAVE results (as shown before) for such sources. One additional result in Gica et al.'s (2008) work, which is important for our simulations, is their sensitivity analysis of tsunami generation to earthquake source parameters. They found that variations in earthquake epicenter location and magnitude were relatively more important for tsunami generation than changes in dip angle, rake angle, average slip value, and fault area. Hence, to a first order, tsunami generation depends more on the average location where the total seismic energy is released and less on the details of the geological parameters affecting this release. This should be even truer in the far-field, where small differences in tsunami waves near the source area should be attenuated.

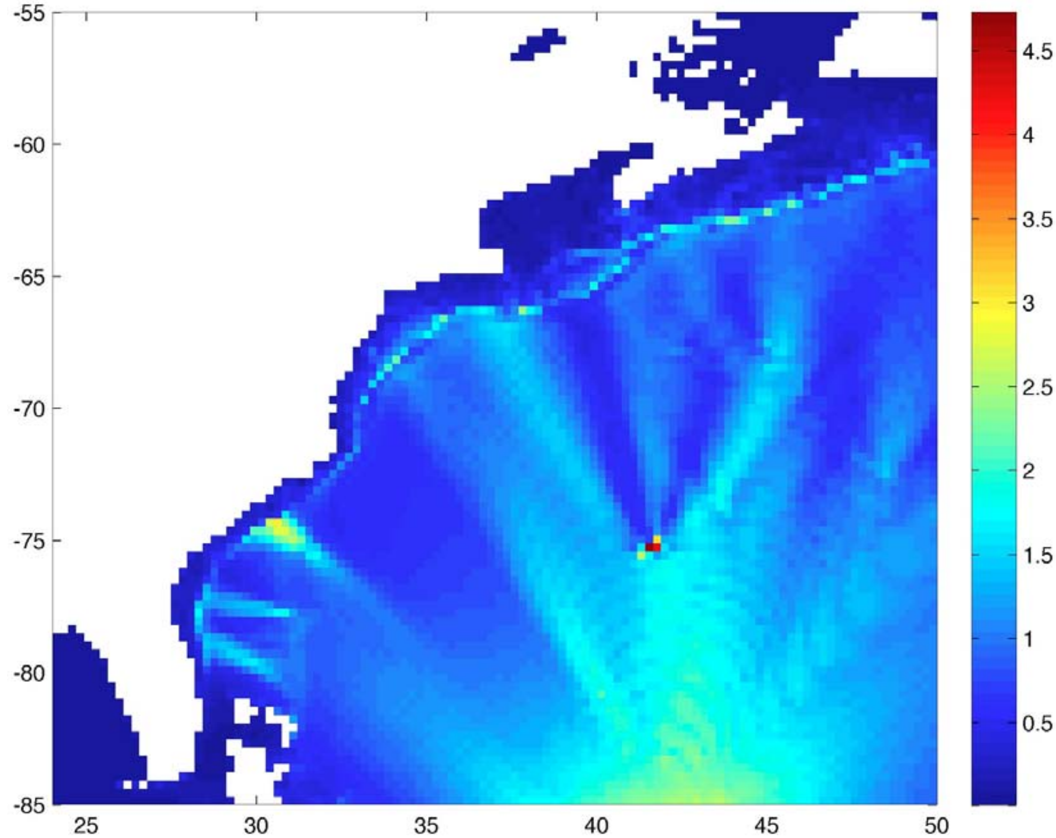

Fig. 7: Ma imum a e height (cm) in NW Atlantic basin, off of the U.S (N Lat-W Long. coordinates). East coast as modeled for NOAA Forecast Source Database unit slip surce case *atszb49* (centered at 19.3859° N 64.7814° W, ith a strike angle of 94.34°, a dip angle of 20.00°, and a depth of 5.00 km).

2.2.3 Azores-Gibraltar convergence zone

The other main source of co-seismic tsunamis in the Atlantic basin is the Azores-Gibraltar con ergence zone (see Fig. 8 and bath metr in Fig. 9). There are se eral potentiall acti e faults in this con ergence zone, including the Gorringe Bank Fault, the Marque de Pombal Fault, the St. Vincente Fault, and the Horseshoe Fault (Fig. 8). Collecti el these faults are considered to be the source of some of the largest historical earthquakes and tsunamis in the Atlantic ocean, including the de astating Lisbon 1755 M_w = 8.5-9 magnitude earthquake and tsunami, hich caused up to 100,000 deaths and generated 5-10 m initial surface ele ations (Baptista et al., 1998a,b; Gutscher et al., 2006), ielding some significant tsunami runup as far as North America. In the far field, Lockridge et al. (2002) reported on the 1755 tsunami runup in the Caribbean. Antigua, Saba, and St. Martin at the northeast corner of the Caribbean Sea had the highest runup, but flooding as also reported from Santiago de Cuba and Samana Ba , Dominican Republic, in the North to Barbados in the south, as ell as north of St. Johns, Ne foundland, but there are no reports of flooding an here else bet een Cuba and Ne foundland, despite the presence at that time of population centers in lo -l ing areas of the rn U.S. and Canada (ten Brink, 2007, 2008). As the nt AA Forecast Source tabase does not include potential distant sources e res-Gibraltar con er e zone, e ill estimate their parameters based on th ting erature.

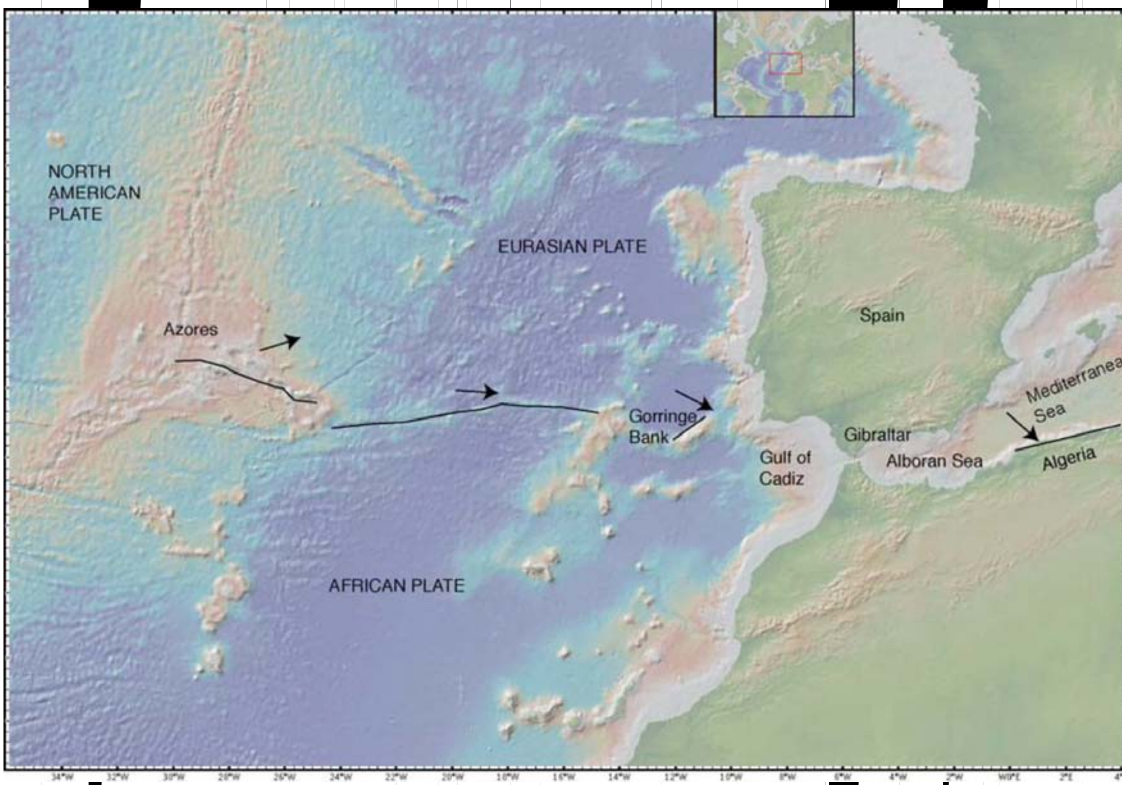

Fig. 8: eod namics of and boundaries bet een the African and Eurasian pla s, near the Azores-Gibraltar con rgence zone. The relati e motion of the Eurasian plate relati e to the frican plate is 4 mm/ ear (from ten Brink, 2007). Some of the major potentiall acti e faults ar sho n on the figure.

The boundar bet een the large African and Eurasian plates e tends from the Azores Triple Junction in the est to the area SW of the Iberia Peninsula. The relati e plate motion is strike-slip, ith a slight di ergence at the estern end near the Azores and con ergence near its eastern end, a modest 4 mm/ ear (Fig. 8, .g., Argus *et al.*, 1989). The ju taposition of t o old and dense plates along the easter end does not allo for subduction to de elop (e.g., Grimison and Chen, 1986). Instead, a zone of diffuse compressi e deformation has de eloped, ith Gorringe Bank and other lesser banks and seamounts, being separated b ab ssal plains of great depth (Fig. 9; Ha ard *et al.*, 1999). Ten Brink et al. (2007, 2008) report that four large tsunamigenic earthquakes ha e occurred in the Atlantic Ocean est of Gibraltar in the last 300 ears: (i) the 1722 (Baptista and Lemos, 2000); (ii) the M_w = 8.5-9 Lisbon 1755 (e.g., Johnston, 1996; Baptista et al., 1998a,b; Gutscher et al., 2006; Grandin et al., 2007); (iii) the 1761 (Baptista *et al.*, 1998); and (i) the M_w = 7.8 1969 (Johnston, 1996) earthquakes. Ho e er, there is no simple tectonic model for this area that e plains the generation of these earthquakes. While it is not clear hich faults are presentl acti e in the region, the fact that an earthquake (and tsunami) as large as that of 1755 could be generated in this area, shows that this event deserves further analysis in the context of the present study.

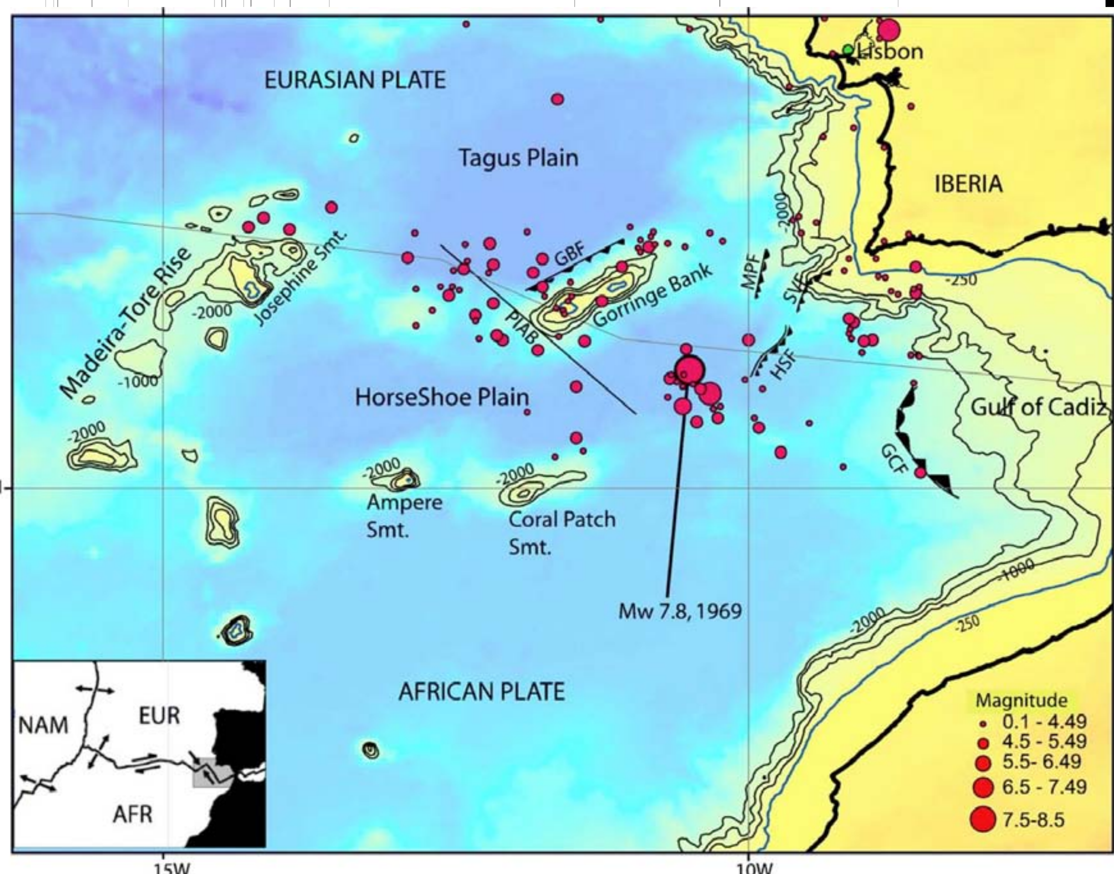

Fig. 9: Area around the Azores-Gibraltar convergence zone, including locations of past earthquake epicenters, as well as proposed faults from previous studies (GBF – Gorringe Bank Fault; MPF – Marques de Pombal Fault; SVF – St. Vincente Fault; HSF – Horseshoe Fault; GCF – Gulf of Cadiz Fault), and the Paleo Iberia – Africa Plate boundary. From Barkan et al. (2009).

As indicated, there is no clear consensus on the location and parameters of the Lisbon 1755 earthquake and tsunami source. Johnston (1996) assumed that Gorringe Bank, which is the major morphologic feature off of Lisbon, rising from a depth of 4,000 m to 25 m (Figs. 8, 9), was the source of the November 1, 1755 Lisbon Earthquake. The same work concluded that the M_w = 7.9 1969 earthquake occurred on a fault parallel to the Gorringe escarpment, but 90 km to the SE. The strike directions of the escarpment and the earthquake were 45°-50° and slip of the 1969 earthquake was to the NW. Johnston proposed the following parameters for the 1755 Lisbon earthquake source: 200 km length, 80 km width, 40° dip angle, 62° strike angle, 332° slip angle, 12 m average slip (the rock density was further selected as 3,330 kg/m^3 with a shear modulus $\mu = 6.5 \times 10^{11}$ dyne/cm^2). By contrast, Gracia et al. (2003) proposed that the 1755 Lisbon earthquake occurred on two other thrust faults (Marques de Pombal fault and Horseshoe-San Vincente fault). These faults have an average strike of 20° and their suggested slip direction was to the NW. Gutscher et al. (2006) attribute the 1755 earthquake to thrusting and subduction of the Eastern Atlantic under the Alboran Sea. The a erage dimensions of their NS oriented fault plane are: 180 km length and 210 km idth. Moment magnitudes ere calculated for t o a erage co-seismic slips of 20 and 10 m using $\mu = 3 \quad 10^{10}$ Pa, ielding M_w = 8.8 and 8.64, respecti el . According to the authors, such an earthquake ould ha e a 1,000-2,000 ear return period.

The Lisbon 1755 earthquake as highl tsunamigenic, and its far-field tsunami impact (including on the North American coast) as modeled b Baptista et al. (1998a,b), Mader (2001) and Barkan et al. (2009). Such studies can be useful not just for understanding tsunami hazard itself, but also for constraining the tsunami earthquake source. Thus, Baptista et al. (1998a,b) performed in erse ra tracing using near-field coastal tsunami obser ations, ielding an optimal location for the 1755 earthquake source as a composite rupture along the SW Iberian coast, ith strikes of 160° and 135°. Barkan et al. (2009), after simulating se eral possible sources, suggested that the 1755 earthquake as generated in the Horseshoe Plain area. It should be noted that other sources selected in the same area, in the same stud , hile not as closel matching the historical records of the generated tsunami, ere sho n to cause a tsunami that could reach the coast of Florida. According to ten Brink (2007), if one assumes that the highest obser ed runup as in the direction of fault slip, then the slip azimuth from the Gulf of Cadiz to Saba is 263°, and if the fault strike is perpendicular to slip then the fault strike as 173°. This fault strike is compatible ith the fault strikes proposed b Baptista *et al.* (1998a,b) and Gutscher *et al.* (2006) and is incompatible ith the sources proposed at Gorringe Bank (Johnston, 1996).

Fault parameters	**Gulf of Cadiz**	**Step-over**	**Marques de Pombal**
Epicenter	35.441°N 8.614°W	36.7310°N 9.2155°W	37.410°N 9.647°W
Strike (degrees)	343	285	330
Dip (degrees)	49.4	24.8	26.1
Rake (degrees)	5	25	25
Ma . slip (m)	20	15	15
Fault depth (km)	10.0	12.7	11.0
Length (km)	180	130	100
Width (km)	210	60	50
Dela (s)	0.0	51.67	89.67

Table 3: Okada's parameters for Lisbon 1755 earthquake faults used b Watts (2006).

A similar case stud of the 1755 tsunami as conducted b Watts (2006), ith the goal of reproducing the near-field obser ations. Based on ground motion and geological interpretation b Risk Management Solutions, Inc., three different tsunami sources ere identified (Table 3; note the shear modulus used as ne er specified), hich ere used to initialize the tsunami propagation model FUNWAVE, using TOPICS. This preliminar ork as able to establish that the fault rupture most likel happened from the south to the north. From his simulated results, Watts as able to get g od agreement ith obser ed runup at most locations. The most notab fference as th t lo runup as predicted at some locations, as compared bser ations, s ggesting that perhaps a local landslide tsunami ma ha e been ered b the e rthquake as ell

2 3 Cumbre Vieja Volcano flank collapse

A other distant tsunami source that could affect the U.S. East coast o be caused b t e potential lateral collapse of the Cumbre Vieja Volcano (CVV) on Palma, in the C anar Islands (Fig. 10). Since the pioneering, but contro ersial, ork Vard and Da (2001), the potential CVV flank collapse has been the object of numerou unami hazard s udies, in particular, regarding the U.S. East coast. Indeed, Ward and assumed an e treme scenario for the estern flank collapse, in ol ing a olume o bout 500 km^3 (ith a 15-20 km idth and a 15-25 km length) and found that such a ass, sliding at speeds up to 100 m/s into the deep ocean, ould generate initial a ith height in e cess of 1 km. Such large a es ould propagate across the Atl ic Ocean and se erel impact distant shores. Based on their highl idealized source d calculations (using a superposition of linear a es), Ward and Da concluded that r field tsunami a es ould cause a 10 to 25 meter runup along the US East coas from North to South).

Fig. 10: Cumbre Vieja olcano (CVV) in La Palma (Canar Islands .

Ward and Da 's catastrophic subaerial landslide scenario and a e modeling approach ere se erel criticized in later ork (e.g., Mader, 2001; or Pararas-Cara annis, 2002; W nn and Masson, 2003). Mader (2001), for instance, performed simulations of the tsunami that ould be produced b the same e treme 500 km^3 scenario, using the Na ier-Stokes (NS) a e model SWAN, and found an order of magnitude smaller a es in the far field than Ward and Da 's. Mader's simulations indicated that up to 3 m high tsunami a es could reach the U.S. East coast for such an e ent. A more rigorous modeling of the slide e ent and a e propagation as done b Gisler et al. (2006) and Lø holt *et al.* (2008), on the basis of a multi-material NS model for the slide and a dispersi e Boussinesq equation model for tsunami propagation, hich confirmed r criticism. Usi smaller 375 km^3 scena , t e simulations predicted si ant a e dispersi nd amplitude deca propor nal the in erse of the distance e source. In the fa d, the predicted up to a 0. m e amplitude in Florida (i.e .6 m height), bu er areas of the U.S. East oas could be more impacted (t some hat consist ith Mader's predictions). N te, f completeness, that Grilli e (2006) and Pérign (2006) had also performed earli simulations of CVV flank apse scenarios, us a dispersi e Boussinesq m del UNWAVE) to simulate tsu i propagation, but mpler semi-empirical suba ial l dslide tsunami source (Wa *et al.*, 2003). The p ietar nature of this ork, h e , had pre ented its publicati ntil recentl .

Geo cal studies ere als oti ated b Ward and Da s (20 1) ork. Thus, Masson et a 2002, 2006) found dences of past large paleo-s bma ne landslides of olume 50- km^3, around the C r Islands, at least demonst ating that such e ents ere not pu speculati e. The nd an a erage recurrence pe iod f r 15 such e ents of *O*(100,00 ears. Ho e er, tur te deposits indicate that such large slides ma ha e occurred in etrogressi e a , h ould ha e reduced their tsunam igenic potential. McMurtr . (2007) found an a ormall high ele ation of a cient marine sediment deposits in path of Ward and 's and others' calculated a es, hich ould be consistent a large tsunami. He , if on the one hand the alarming ork of Ward and Da (2001) a be subject to cri isms as documented in subsequent ork re ie ed abo e, on t other hand, the lack kno ledge regarding such e treme natural hazards and related unami phenomena, rrants further anal sis in the conte t of the present ork.

Hen , in a separate task of his NHTMP project, e perform ne simulations of CVV flank ollapse scenarios, usi g the incompressible multi-fluid 3D-NS Volume Of Fluid (VOF model (referred to as HETIS; e.g., Abadie et al., 2010). THETIS' output is used as an itial condition for th (full nonlinear and dispersi e) Boussinesq model FUNWAVE in hich e perform simulations of transoceanic tsunami propagation and impact on e U.S. East coast, i a series of nested model grids. Regarding CVV landslide sc arios, follo ing the i itial ork of Abadie et al. (2008), these are based on ne slope s bilit anal zes of the CVV estern flank, conducted as part of the European research pr ect TRANSFER (Fab e et al., in re ision). In these studies, potential failure surfaces ar inferred from field data, laborator tests, and slope stabilit anal ses performed n a series of 2D ertical slices (in the olcano estern flank), using t o different nu merical models, based on a Mohr-Coulomb failure criterion. The likeliest failure surf ce is identified b graduall decreasing material propert alues (thus mimicking drothermal alteration of the CVV flank). A global shear zone, more or less parallel to the topograph and dipping 24° est ard, as thus identified, based on global plastic indicators and areas of ma imum shear strain. On this basis, a 2D slide cross-section as finall defined, hich allo s calculating slide olume based on field data (idth and length of semi-elliptic shape). Doing so, Fabre et al. estimated potential CVV landslide olumes ranging bet een 38 and 68 km^3, depending on the h potheses made on the lateral e tent of an gi en failure. These alues, hich are much smaller than the 500 km^3 olume proposed b Ward and Da (2001) (and later used in Gisler et al. 2006, and

Lø holt et al. 2008), appear to be more reasonable in ie of the size of deep ater deposits identified at the toe of the olcano, possibl corresponding to the CVV last massi e flank collapse (about 300,000 ears ago).

In summar , slide olumes of 38 to 68 km^3 ill be used in the present NTHMP CVV modeling studies, but the 500 km^3 scenario ill still be simulated to compare our results ith Lø holt et al.'s (2008). Note, ho e er, that the high safet factors found in Fabre et al.'s anal ses indicate that the CVV estern flank is rather stable under present conditions. Large seismicit and/or a olcanic eruption could ne ertheless pro ide additional destabilizing forces that ere not included in their anal ses.

3. INITIAL SOURCE DEFINITI AND TSUNAMI SIMULATIONS

3.1 Modeling methodology

Tsunami propagation simulations be performed for a series of tsunami sources, the Boussinesq model FUNWA , either in its original full nonlinear Cart implementation, for the finer re al nearshore grids (see Wei et al., 1995; Wei Kirb , 1995), or in its m recent eakl nonlinear spherical coordi implementation, for the ocean ba scale grids (Kirb et al., 2009). The full nonl model is based on a second-ord eries e pansion of the ertical ariation in el potential. Unlike the Nonlinear llo Water (NSW) equations, traditionall use stud ing tsunami propagation a coastal impact, the Boussinesq approach incl s dispersi e effects, hich ma b ignificant for landslide tsunami sources and a t tsunami propagation and runup t ugh a e- a e interactions. To simulate both e breaking and inundation o er dr nd, FUNWAVE has a parameterization of turb nt dissipation and bottom friction. ts more recent implementation, FUNWAVE (h er Cartesian or spherical) has been allelized using the MPI language (Pophet, 2008). he code as thus sho n to be er fficient and highl scalable on small to medium ze computer clusters (Pophet et al. 010). These recent parallel ersions of FUNW E ill be used for modeling tsunam in the present cases of interest.

3.1.1 Initial conditions for mo el

In earlier tsunami modeling stud s, FUNWAVE has been combined ith a preproc sor that generates arious tsunami urces (e.g., co-seismic, landslide,…), the "Tsu mi Open and Progressi e Initial Co ditions S stem" (TOPICS; see Watts et al., 2003). The FUNWAVE-TOPICS combinati n, referred to as GEOWAVE, has been alidated sed on historical case studies of unde ater landslide tsunamis (e.g., Watts et al., 2003; er et al., 2004; Da et al., 2005; G eene et al., 2006; Rahiman et al., 2007; Tappin e al., 2008), earthquake generated tsu amis (Da et al., 2005; Grilli et al., 2007; Ioualal n et al., 2006; 2007), and debris flo (Walder et al., 2006; Wa thomas et al., 2006). A he ersion of the tsunami source pr processor, hich both as implemented in a more ser-friendl MATLAB (GUI) e ironment and hose landslide tsunami s urce parameterization as updated (se later) ill be used in the present simulations.

3.1.2 Co-seismic sources

The standard idealized Okada (1985) method ill be used to model co-seismic tsunami sources, as detailed in Appendi A.1. This procedure ields an initial ocean surface ele ation, based on the earthquake location, moment magnitude, geographic e tent (length, idth) and depth, and geological parameters (shear modulus, fault plane dip, strike and rake angles). Note that the slight modification of Okada's method introduced in the original TOPICS ill be used here. As summarized in Appendi A.1, this simpl allo s spec f ing a some hat more realistic Gaussian-like distribution of slip ithin the fault plane.

3.1.3 Submarine mass failures

As planned at the onset of this project, tsunami hazard resulting from potential Submarine Mass Failures (SMFs) along the US east coast, from Florida to Maine, ill first be studied using Monte Carlo Simulations (MCS), based on the probabilistic slope stabilit anal ses of Grilli et al. (2009). This ill allo defining and parameterizing a series of potential slope failures (slides or slumps), for hich SMF tsunami sources ill be de eloped and FUNWAVE simulations performed, follo ing the methodolog outlined in Watts et al.'s (2003, 2005). These sources, hich are detailed in Appendi A.2, are based on semi-empirical (cur e) fits deri ed from a large number of full 3D SMF tsunami generation simulations (Grilli et al., 2002; Grilli and Watts, 1999, 2005; Watts et al., 2005). SMF tsunami source parameters are based on the slide specific densit , landslide length, ma imum thickness and idth, mean initial depth, and mean initial incline angle, as ell as the location and angle (direction) of the landslide.

3.1.4 Subaerial landslide sources

As discussed abo e for the CVV case stud , tsunami generation b subaerial landslides ill be modeled using the 3D-Na ier-Stokes model THETIS (Abadie et al., 2009, 2010, 2011), hich sol es for the elocit and pressure of all three phases: ater, air, and landslide. Similar to the model coupling of Lø holt et al. (2008) for the CVV case, THETIS ill be coupled to FUNWAVE to simulate the 2D-horizontal ocean-scale tsunami propagation and coastal impact. Specificall , in this one- a model coupling approach, THETIS is used to simulate the first fe minutes (10 mins. or so) of the subaerial e ent and initial (near-field) tsunami generation that results. FUNWAVE is then initialized ith the calculated sea surface height and depth-a eraged horizontal elocit to perform far-field simulations.

3.2 Sources

3.2.1 Submarine mass failures

For the purposes of modeling SMFs tsunamis along the U.S. East coast, as indicated, most sources ill be deri ed from a separate MCS anal sis. Additionall , specific SMF sources ill be designed based on the best a ailable data (see Table 4) and used to simulate tsunamis generated b t o ell-kno n large under ater landslides, off of the US East coast : (i) the Currituck, and the Grand Banks 1929, landslides. Fig. 4 sho s a preliminar simulation of the initial stages of tsunami propagation for case (i).

Parameter	Grand Banks (1929)	Currituck landslide
Location	44.691° N 56.006° W	36.5° N 74.5° W
Direction	170°	100°
Slope incline	6°	4°
Bulk densit	2,000 kg/m^3	2,000 kg/m^3
Thickness	5 m	250 m
Length	135 km	30 km
Width	260 km	20 km
Water depth	1,687 m	

Table 4: List of parameters for designing tsunami sources for t o past SMFs.

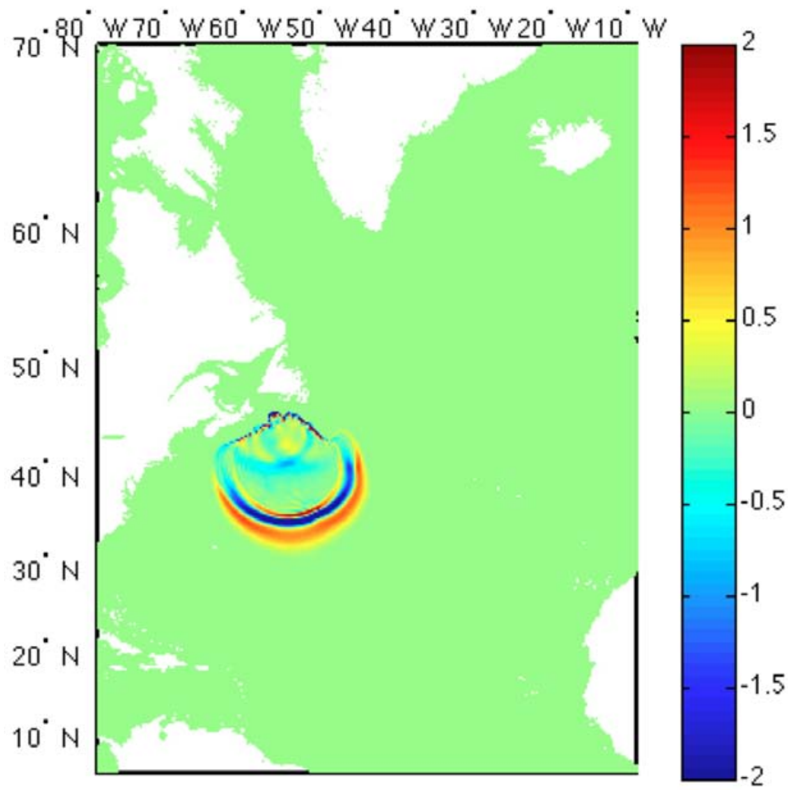

Fig. 11: FUNWAVE simulation of tsunami ele ation (m) caused b a SMF similar to the Grand Banks 1929 e ent. Parameters of the slide are gi en in Table 4.

3.2.2 Co-seismic tsunamis

Co-seismic tsunami sources ith the potential to cause tsunami hazard along the US East Coast ha e been identified in t o areas : (i) the Caribbean subduction zone; and (ii) in the Azores con ergence zone.

Regarding area (i), if e focus on earthquakes in the Puerto Rico Trench (PRT) as the most likel sources of tsunami generation, a preliminar list of potential sources ould be a ailable from both historical e ents and predicted earthquake parameters based on plate con ergence rates and other kno n geological information (e.g., Mercado and McCann, 2001; Grilli et. al., 2010a). Table 5 summarizes selected sets of geological parameters for tsunamigenic earthquakes around the PRT. The first 12 sets are identical to sources 48-53, *a* and *b*, of the NOAA Forecast Source Database, and the remaining sets are e amples that could be used to test the sensiti it of tsunami generation to arious parameters.

Longitude	Latitude	Strike Angle	Dip Angle	Depth (km)
-63.8800	18.8870	95.37	20.00	21.10
-63.8382	19.3072	95.37	20.00	5.00
-64.8153	18.9650	94.34	20.00	22.10
-64.7814	19.3859	94.34	20.00	5.00
-65.6921	18.9848	89.59	20.00	22.10
-65.6953	19.4069	89.59	20.00	5.00
-66.5742	18.9484	84.98	20.00	22.10
-66.6133	19.3688	84.98	20.00	5.00
-67.5412	18.8738	85.87	20.00	22.10
-67.5734	19.2948	85.87	20.00	5.00
-67.4547	18.7853	83.64	20.00	22.10
-68.5042	19.2048	83.64	20.00	5.00
-66.6133	19.3688	94.98	20.00	5.00
-66.6133	19.3688	74.98	20.00	5.00
-66.6133	19.3688	84.98	10.00	5.00

Table 5: Geological parameters for potential co-seismic tsunami sources in the PRT.

Magnitude (M_W)	Moment M_0 (Nm)	Area $A(km^2)$	Length L(km)	Width W(km)	Slip Δu(m)
6.5	6.3 10^{18}	224	28	8	.56
7.0	3.5 10^{19}	708	50	14	1.00
7.5	2.0 10^{20}	2,239	89	25	1.78
8.0	1.1 10^{21}	7,079	158	45	3.17
8.5	6.3 10^{21}	22,387	282	79	5.66
9.0	3.5 10^{22}	70,794	501	141	10.0
9.5	2.0 10^{23}	223,872	891	251	17.8

Table 6: Relationship bet een different parameters for tsunamigenic earthquakes (Ward, 2001).

Table 5 does not include e ents magnitude and area (i.e., length and idth), from hich an a erage fault slip can be obtained. In the absence of more detailed information, Ward (2001) defined t pical relationships bet een earthquake parameters (Table 6), hich could be useful for designing sources.

Fig. 12 sho s a t pical simulation ith FU[illegible]AVE o[illegible] genera[illegible] and earl propagation of an e treme co-seismic tsunami [illegible]e PRT, [illegible] geolog[illegible] parameters are identical to those modeled b Grilli et al. (2[illegible]a) (Table[illegible]e., loca[illegible]: 19.674° N 65.806° W, strike 92°, dip 15°, rake 50°, dept[illegible] km, len[illegible]00 km, [illegible]dth 150 km, e cept for an a erage slip 16.7 m (corresponding[illegible]agnitude [illegible]9.1) an[illegible]ear modulus 4.2 10^{10} Pa (deca radius 200 km, depth of slip [illegible] m, and [illegible]depth 7,[illegible] m).

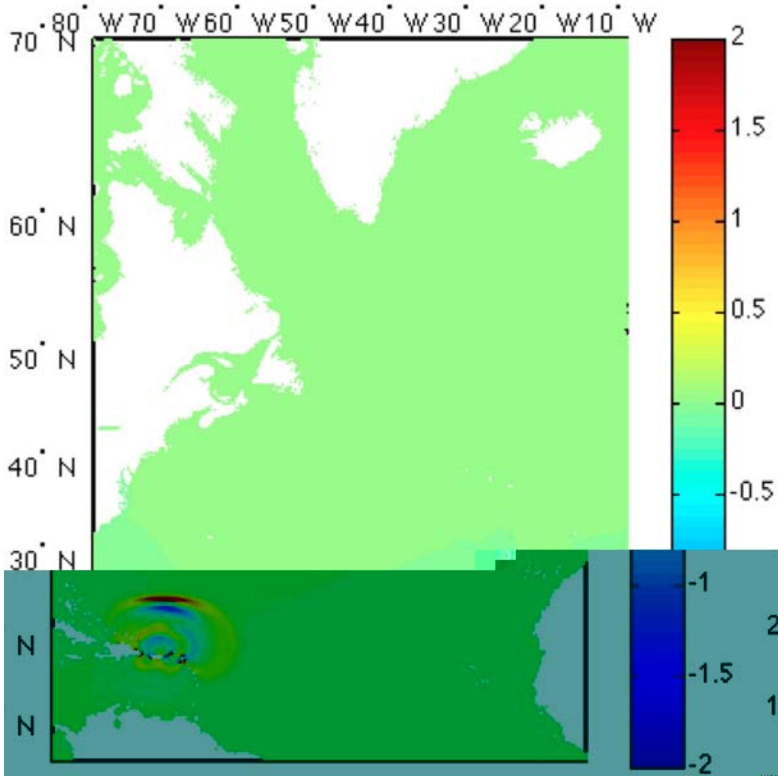

Fig. 12: FUNWAVE simulation of tsunami ele ation (m) caused b a earthquake in the PRT, ith geological parameters identical to those modeled b Grilli et al. (2010a) Table 2). Location: 19.674° N 65.806° W, strike 92°, dip 15°, rake 50°, depth 40 km, length 600 km, dth 150 km, e cept for a erage slip 16.7 m (magnitude M_w = 9.1) and shear modulus 4.2 10^{10} Pa (deca adius 200 km, depth of slip 400 m, and ater depth 7,000 m).

Regarding area (ii), hich is the source of the largest kno n earthquakes and tsunamis in the north Atlantic basin, a thrust fault ith rake of 90° ill be used, hich results in the highest possible transoceanic tsunami a es (Geist, 1999). Based on ten Brink et al. (2008), a fault strike of 345°, hich ields the highest amplitudes in the Caribbean Coasts, ill be considered. ten Brink et al. further assumed in their modeling: a dip of 40º, rake of 90º, a source depth of 5 km, fault length of 200 km, idth of 80 km, and an a erage slip 13.1 m (hich assuming a shear modulus of 6.5 10^{10} Pa ields a magnitude M_w = 8.7). Table 7 specifies selected location of arious potential co-seismic sources.

Lat.	35.48	36.21	35.14	37.15	36.04	37.04	36.94	36.01	37.95
Long.	-8.2	-9.82	-10.05	-10.11	-10.75	-10.78	-11.45	-11.46	-12.05

Table 7: Potential earthquake epicenters for the Azores-Gibraltar [illegible] oundar (ten Br[illegible]. al., [illegible]

Fig. 13 sho s a t pical simulation ith FUNWA[illegible]f the genera[illegible] and [illegible] propagation of an e treme co-seismic tsunami gener[illegible]b a source [illegible] geo[illegible]al parameters (as discussed abo e) similar to those [illegible]n (estimated) [illegible]sbon [illegible]55 earthquake, i.e., location: 36.015° N 11.467° W, strike [illegible]°, dip 40°, rak[illegible]°, de[illegible]30 km, length 200 km, idth 80 km, shear modulus 6[illegible]0^{10} Pa, a erag[illegible]slip 1[illegible]m (corresponding magnitude M_w = 8.7), radius 300 km[illegible]th of slip 40 [illegible], and[illegible]er depth 4,709 m.

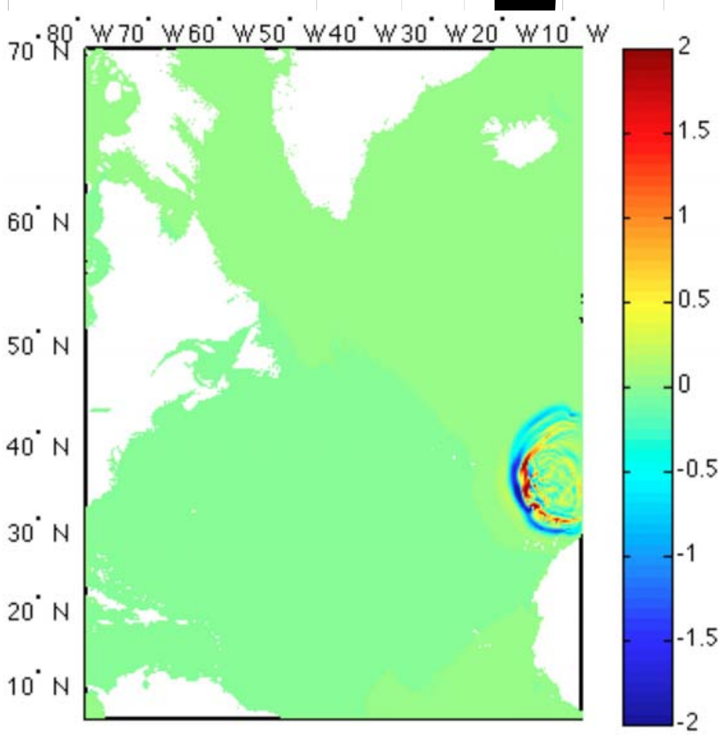

Fig. 13: FUNWAVE simulation of tsunami ele ation (m) ca[illegible]ed b an earthquake similar to t[illegible]e (estimated) 1755 Lisbon e ent. Location: 36.015° N 11.467° W, [illegible]rike 345°, dip 40°, rake 90°, ma[illegible]nitude 8.7, a erage slip 13.1 m, depth 30 km, length 200 km, idth 80[illegible]m, shear modulus 6.5 10^{10} Pa ([illegible]eca radius 300 km, depth of slip 40 km, and a[illegible]r depth 4,709 m).

In the preliminar simulations of both Figs 12 and 13, e see significant tsunami a es propagating to ards the US East coast.

3.2.3 Cumbre Vieja Volcano flank collapse

The Cumbria Vieja Volcano (CVV) flank collapse has been identified as an e treme subaerial landslide tsunami source in the Atlantic Ocean basin, ith the potential to generate er high and steep near-field a es and significant far-field a es along the US East Coast. As indicated earlier, due to the comple it of both the source mechanism and the flo in near field a es, the 3D multi-material Na ier-Stokes sol er THETIS is used to generate the initial conditions, in a fine local grid. As an illustration, Fig. 14 sho s snapshots of   ater and slide interfaces at times up to 10 minutes (olume fractions respecti el   equal to 0.5 and 0.1) from THETIS' simulation of a subaerial landslide tsunami resulting from a CVV flank collapse scenario,   ith an initial slide   olume of 80 km^3.

In the case of the CVV, as it   ould be prohibiti e to run FUNWAVE   ith a structured grid that both resol es the island of La Palma and the entire North Atlantic at the same time, this coupling process is duplicated   ithin FUNWAVE, i.e., a regional Cartesian grid (e.g., 15"   15") is first used directl   around La Palma, to perform tsunami simulations based on THETIS source (e.g., at 10 mins., see Fig. 14c), for the first half hour or so of time, at   hich point results are sa ed and re-interpolated onto a coarser spherical grid (e.g., 2'   2') o er the entire North Atlantic Ocean,   hich is then used to perform FUNWAVE simulations of trans-Atlantic tsunami propagation.

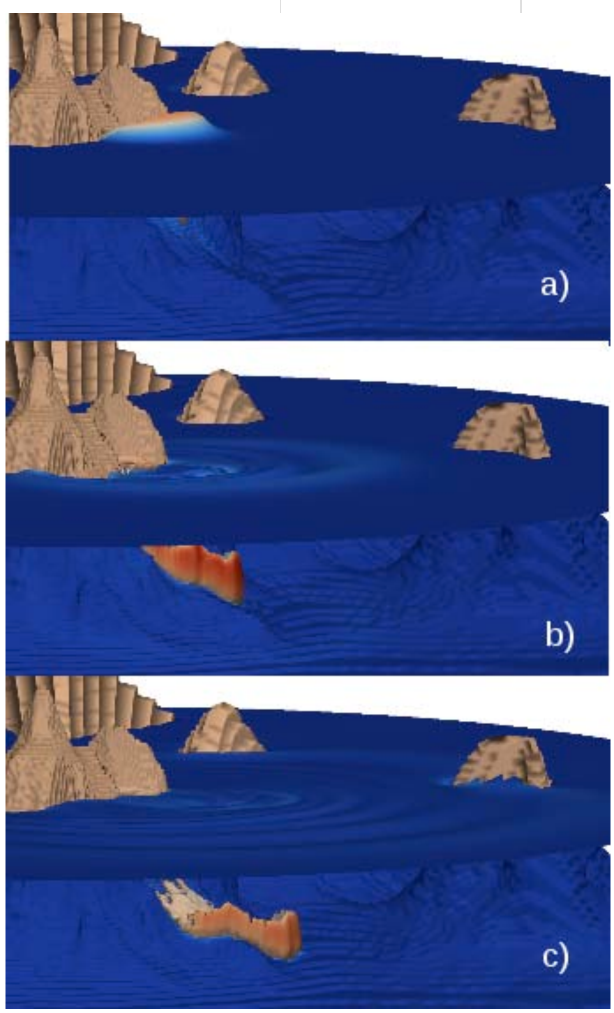

Fig. 14 : THETIS simulation of subaerial landslide tsunami generation b   a CVV flank collapse scenario   ith a slide initial   olume of 80 km^3. Snapshots of   ater and slide interfaces (olume fractions respecti el   equal to 0.5 and 0.1) at t=: a) 2 min, b) 6 min, c) 10 min into the e ent.

This is illustrated in Figs. 15 and 16. Fig. 15 sho s results in the regional 15” grid, resol ing a es directl around La Palma at time t = 25 mins., and Fig. 16 sho s propagation at time t =5h33’, in the 2’ trans-Atlantic grid. Note, in the latter preliminar simulations, some artifacts of the model lo er boundar condition (sponge la er) are isible as spurious reflection, lo er than 15deg. N latitude. These a es, ho e er, ould not affect results along the US East Coast and could be easil eliminated b idening the lo er boundar sponge la er.

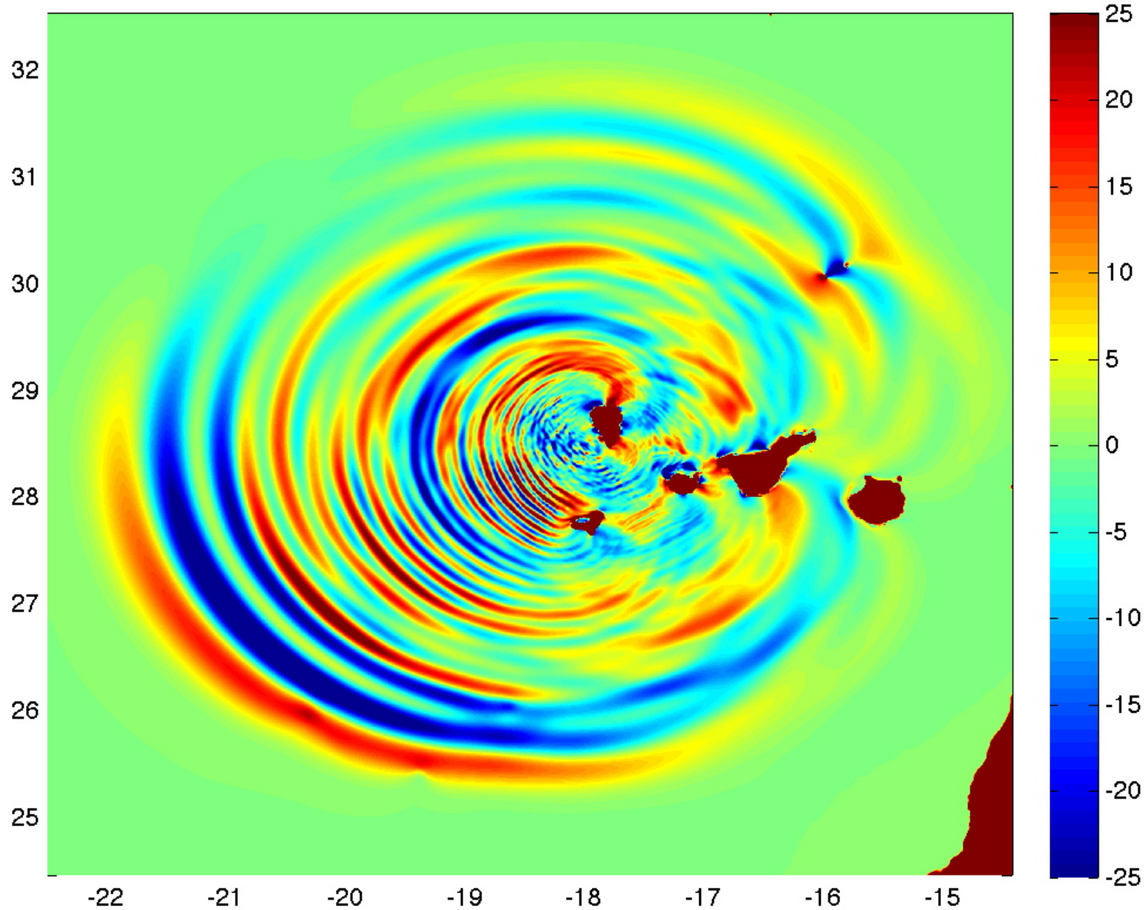

Fig. 15: Case of Fig. 14. (Cartesian) FUNWAVE simulation of tsunami ele ation (m) at time t = 25 min, in a regional 15” grid, initialized at t = 512 s using 3D-NS THETIS results (Fig. 14).

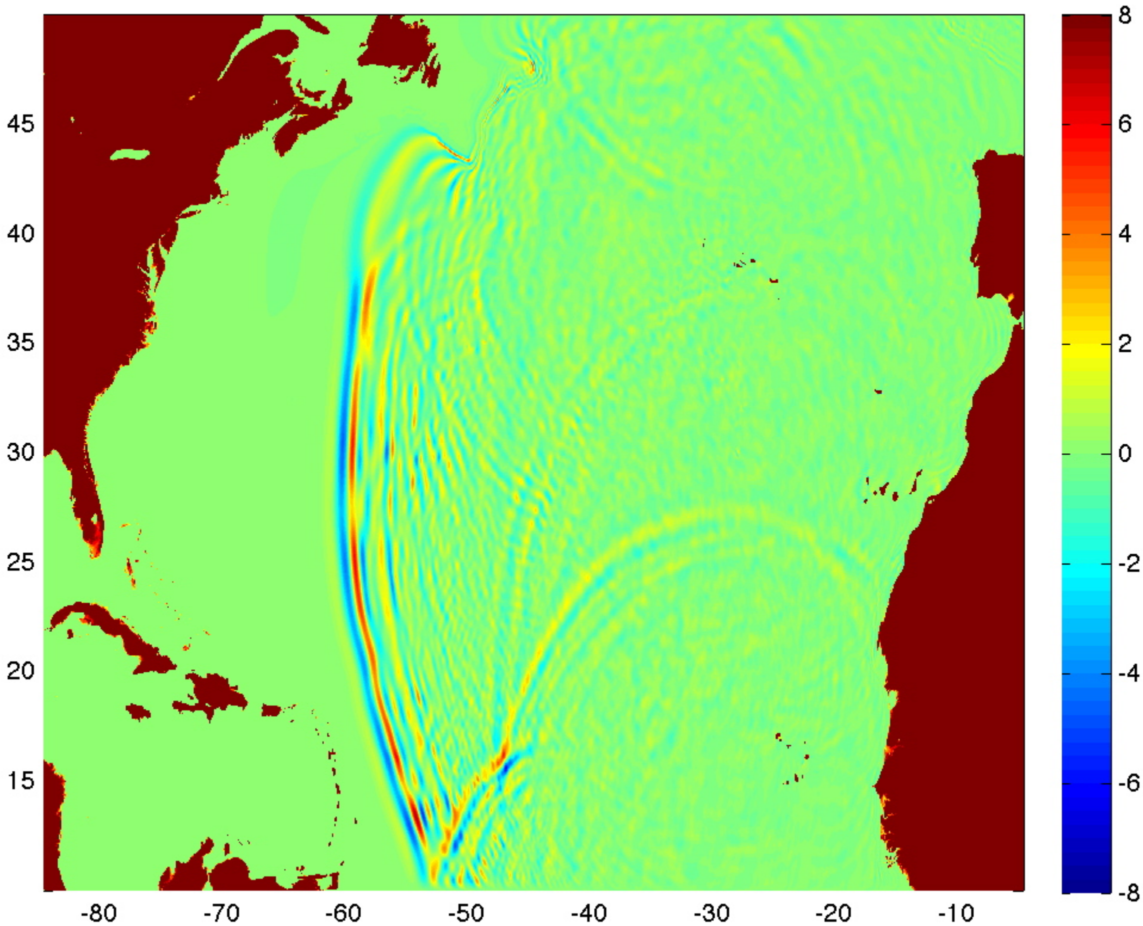

Fig. 16: Case of Figs. 14,15. (Spherical) FUNWAVE simulation of tsunami ele ation (m) at time t = 5h33’, in a basin scale 2’ grid, initialized at t = 25’ using FUNWAVE regional grid results (Fig. 15).

4. SUMMARY

A literature re ie demonstrates that tsunami hazard on the U.S. East coast is still not understood ell, due to the lack of direct obser ations and the paucit of historical records. While less frequent than tsunamis in the Pacific ocean, tsunamis ould ha e the potential to cause e tensi e damage to the densel -populated and lo -l ing cities of the U.S. East coast.

After considering a large number of the likel sources for tsunamis that ould affect the area, including tsunamigenic earthquakes, submarine landslides, and subaerial landslides, a selection of sources as made, for further stud of tsunami generation, propagation and inundation ith the numerical models FUNWAVE and THETIS. FUNWAVE is a Boussinesq model, hich is full nonlinear in its Cartesian implementation and mildl nonlinear in its spherical implementation, for long a e propagation, that has been successfull used and alidated for model tsunami case studies. Further alidation as conducted as part of this NTHMP project alidation orkshop. THETIS is a 3D multi-material Na ier-Stokes model, hich has been alidated for landslide tsunami generation based on standard problems found in the literature (e.g., Russel’s a e generator) and for additional cases as part of this NTHMP project alidation orkshop.

5. APPENDIX A: Implementation of co-seismic and SMF sou s

In this NTHMP funded tsunami hazard and inundation ork, tsuna ropagation and coastal impact simulations are performed using the latest benchma ersion of the full nonlinear Boussinesq long a e model FUNWAVE (Wei et al. 95; Chen et al., 2000; Kenned et al., 2000; Kirb , 2003; Kirb et al., 2009). A prepr ssor, referred to as TOPICS for "Tsunami Open and Progressi e Initial Conditions S s ", is used in the model to set-up and initialize a ariet of tsunami sources, including c eismic and SMF (see, e.g., Watts et al, 2003). A summar of FUNWAVE's equa ns and tsunami implementation can be found in Ioualalen et al. (2007).

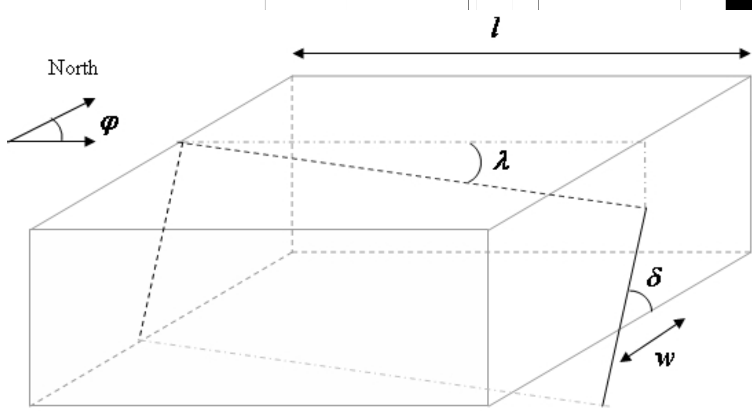

Fig. A1: Sketch of idealized Fault Geometr in Okada's method (1 85).

A.1 Co-seismic sources

The modeling and initialization of co-seismic tsunami sources in OPICS' are based on the standard Okada's (1985) method, ith some minor adjustments hich are detailed belo . Parameters of the method are three angles orienting the "slip fault plane" (strike φ, dip δ, rake λ; Fig. A1), the length l and idth w of the horizontal rectangular rupture area $A = l\,w$ (centered on the slip plane centroid and ith its length oriented in the strike angle direction φ, measured from the geographic North), and material (Lamé) parameters (μ, λ_l). In TOPICS' implementation of Okada's method, ma imum fault slip Δ and a erage slip $\bar{\Delta}$ are obtained from the equation,

$$M_0 = \mu\Delta \int_A f_1 f_2 dx_p dy_p = \mu\bar{\Delta}A \qquad \text{(A1.1)}$$

hich calculates the total energ M_0 [J] released b an earthquake (related to the earthquake magnitude: $M_w = (\log M_o/1.51) - 6$, b Hanks and Kanamori's relationship), here μ and A are input parameters defined abo e, and (f_1, f_2) are t o empirical functions (the form[illegible]g Gaussia[illegible]like) describing [illegible]e assumed shape of the slip distribution ithin the [illegible]ation plane gi en b ,

$$f_1 = \exp\left[\frac{-0.[illegible]931}{[illegible]^2}\left(x_p^2 + y_p^2 + \left(z_p [illegible] D\right)^2\right)\right] \tag{A1.2}$$

$$f_2 = \exp\left[4.6[illegible]52\frac{D_0}{z_p}\right] \tag{A1.3}$$

ith (x_p, y[illegible] the coordinates of points ithin the dislocation plane in UTM coordinates (x_p and y_p[illegible]s are oriented parallel to the sides of the rectangular rupture area and centered [illegible]e centroid of the slip plane). We further note that z_p is zero at the earth surface a[illegible]egati e in the interior, R is the radial distance from the centroid of the rupture ar[illegible]r slip to drop to 50% of its ma imum alue, D_0 is the depth belo hich slip drops [illegible]% of its ma imum alue, and D is the depth of the fault plane centroid. Function f[illegible]o s to concentrate slip near the center of the slip plane and to control slip deca in a[illegible] is mmetric manner from this center, hile Function f_2 allo s specif ing some as [illegible]tr ith depth on the plane, in slip distribution, essentiall b reducing slip in the shal[illegible]er region (ith respect to the control depth D_0).

Fo[illegible] point (x,y) ithin area A (x and y are also oriented parallel to the sides of the rectan[illegible]ar rupture area and centered on the centroid of the slip plane), the ertical seafloor el[illegible]tion is computed as,

$$z(x,y) = -[illegible]\int_A f_1 f_2\left\{\cos\lambda\left(3\xi\zeta\frac{q}{r_0^5} + f_3\sin\delta\right) + \sin\lambda\left(3\zeta\frac{pq}{r_0^5} - f_4\sin\delta\cos\delta\right)\right\}dx_p dy_p \tag{A1.4}$$

ith,

$$[illegible] = x - x_p \;,\; \eta = y - y_p \;,\; \zeta = -z_p \;,\; r_0 = (\xi^2 + \eta^2 + \zeta^2) \tag{A1.5}$$

$$[illegible] = \eta\cos\delta + \zeta\sin\delta \;,\; q = \eta\sin\delta - \zeta\cos\delta$$

$$[illegible] = -\nu\frac{\eta\xi(2r_0 + \zeta)}{r_0^3(r_0 + \zeta)^2} \;,\; f_4 = \frac{\nu}{r_0(r_0 + \zeta)}\left\{1 - \frac{\xi^2(2r_0 + \zeta)}{r_0^2(r_0 + \zeta)}\right\} \tag{A1.6}$$

In TOPIC[illegible], the integrals in Eqs. (1-6) are calculated as sums o er a series of (N x M) panels dis[illegible]etizing the slip plane, ith (x,y,z) denoting the panel center coordinates.

On[illegible]e the seafloor ele ation is calculated, the horizontal coordinates (x,y) are rotated in [illegible]he actual strike direction φ of the rupture area. [This is the reason h strike does not e plicitl appear in Eqs. (4-6).]

Okada's method assumes a locall flat ocean bottom. Ho e er, in tsunami simulations, the actual bottom bath metr is specified in FUNWAVE, hile the tsunami source is e pressed at $t = 0$ as an initial free surface ele ation ith no flo elocit (i.e., cold start).

A.2 S[redacted]sources

The m[redacted]eling and initialization [redacted] Submarine Mass Fail[redacted]SMF) tsunami sources in TOPIC[redacted] are based on the [redacted]or[redacted]f Grilli and Watts (19[redacted]2001, 2005), Grilli et al. (2002)[redacted]atts and Grilli (2003), [redacted]atts et al., (2003, 2005)[redacted]et and Grilli (2003, 2007). The la[redacted] ork deals ith the m[redacted]eling and laborator e[redacted]ments of rigid under ater slides ([redacted]., translational) and slu[redacted]s (i.e., rotational).

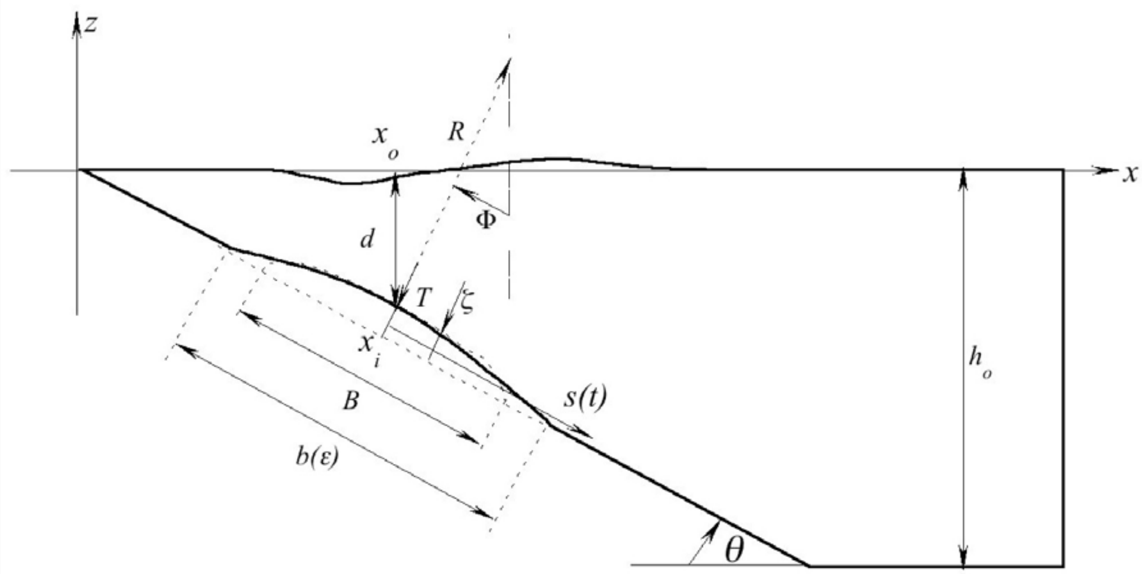

Fig. A2: Parameters definition for 2D cross-section in sli[redacted]e or slump (from Grilli and Watts, 2005)

In this initial computational ork, hich led to T[redacted]PICS, both slides and slump ere first considered as ide rigid bodies of 2D semi-elli[redacted]tical cross-section ith major semi-a is $B/2$ and minor semi-a is T (idth $w >> B$), sli[redacted]ing on a plane slope of angle θ in a fluid of densit ρ_w (Fig. A2; Grilli and Watts, 199[redacted], 2005). The landslide has an a erage bulk densit ρ_b, and its middle location on th[redacted] slope is initiall located at abscissa x_i. Hence,

$$x_i = x_o - T\sin\theta \quad \text{with} \quad x_o = \left(d + \frac{T}{\cos\theta}\right)\frac{1}{\tan\theta} \qquad \text{(A2.1)}$$

here x_o is the abscissa on the slope of the location of ma imum thickness on the slope. Once the slide motion has been triggered (e.g., b an earthquake), it is assumed that basal friction bet een slide and slope is negligible and that friction is limited to a global h drod namic drag force (ith drag coefficient C_d) acting on the slide cross section. Similarl , ater inertia effects are represented b a global added mass (ith added mass coefficient C_d). For such 2D bodies, the olume and cross-section are simpl ,

$$V_s = \frac{\pi}{4}wBT \quad \text{with} \quad A_s = wT \qquad \text{(A2.2)}$$

A.2.1 2D u[illegible]derwate[illegible]es

Rig[illegible] translati[illegible]lide motions are mod[illegible] the displacem[illegible]t *s(t)* of their center of m[illegible]s (Fig. A[illegible]hich is found based on [illegible]ilibrium of iner[illegible], added mass, gra it , h [illegible]od namic [illegible] and buo anc forces a[illegible]

$$s(t) [illegible] s_o \ln\left(\cos[illegible] \right) \quad \text{with} \quad s_o = \frac{u_t^2}{a_o} \quad \text{and} [illegible] \frac{u_t}{a_o} \qquad \text{(A2.3)}$$

ith the ini[illegible]al accelera[illegible] and terminal elocit ,

$$a_o [illegible] g\sin\theta\left(\frac{\gamma [illegible]}{\gamma + [illegible]} \right) \quad \text{and} \quad u_t = \left(gB\sin\theta \frac{\pi([illegible]}{2 [illegible]} \right)^{\frac{1}{2}} \qquad \text{(A2.4)}$$

respecti el[illegible], $\gamma = \rho_b/\rho_w$[illegible]d g denoting the gra itati[illegible]acceleration.

For such slides[illegible]rilli and Watts (1999, 20[illegible] performed man 2D simulations, using a full nonlinea[illegible]otential flo model, and [illegible]atts et al. (2005) deri ed a semi-empirical e pression f[illegible]he minimum surface depr[illegible]on η_o computed at $x = x_o$, referred to as the *characteristic[illegible]unami amplitude*, based o[illegible] cases of 2D slide simulations, for arious combinations [illegible]go erning parameters: *B,* [illegible] $\theta, \gamma,$ using appro imate orders of magnitude alues for t[illegible]h drod namic coefficient[illegible] $_d = C_m = 1,$

$$\eta_o = s_o(0.0592 [illegible] .0636\sin\theta + 0.0396\sin^2\theta)\left([illegible] \right)\left(\frac{B\sin\theta}{d} \right)^{1.25} (1 - e^{-2.2(\gamma-1)}) \qquad \text{(A2.5)}$$

This equation predicts[illegible]o er 99% of the ariance [illegible] the computed alues of η_o (R^2 = 0.991) and is based o[illegible] the follo ing ranges of pa[illegible]ameter alues (in non-dimensional form) in the computati[illegible]ns: $\theta \in [5,30]$ deg., $d/B \in [$[illegible]$.06,1.5]$, $T/b \in [0.008,0.2]$, and $\gamma \in [1.46,2.93]$. [Note, [illegible]q. A2.5 has been slightl e [illegible]tended to pro ide higher accurac , as compared to Eq. (2) i[illegible] Watts et al. (2005)]. See Fig[illegible] A3a for a comparison of computed alues of η_o to predicte[illegible] alues from Eq. A2.5, for th[illegible] 32 computed slides.

A.2.2 2D underwate[illegible] slumps

Slumps are modeled as rigid SMFs of ma imum angular displacement $\Delta\phi = \phi - \phi_o$ of their center of mass (Fig. A2). Assuming a nearl circular rupture surface of radius *R* and a small angular displacement (ith $\sin\phi \approx \phi$), the slump translation *s(t)* along the slope (appro imated b the chord of the rupture surface) is found based on an equilibrium of inertia, added mass, gra it , and buo anc forces as,

$$s([illegible] s_o\left(1 [illegible] \cos\left(\frac{t}{t_o}\right) [illegible] \quad \text{s}_o = \frac{\Delta s}{2} \quad [illegible] \quad t_o = \left(\frac{R(\gamma + C_m)}{g(\gamma - 1)}\right) [illegible] \qquad \text{(A2.6)}$$

N[illegible]te, h [illegible] d[illegible] nam[illegible]c fricti[illegible] ha[illegible]en neglect[illegible] n these equations [illegible] use of the lo er s[illegible]ump el[illegible] ties (a[illegible]s compa[illegible]ed t[illegible] des) and b[illegible] Coulomb friction [illegible] n coefficient C_n) is implici[illegible] inclu[illegible]ed in t[illegible]e sp[illegible]ied angul[illegible] splacement; thus, [illegible] ming a circular r[illegible]pture su[illegible]ce of radius of cur[illegible] e R, e fi[illegible]

$$\Delta s [illegible] R(\Delta\phi) = 2RC_n [illegible] os\theta [illegible] \qquad \text{(A2.7)}$$

[illegible]here Δs [illegible] the ma imum s[illegible]lum[illegible] ear displace[illegible]nt and other definit[illegible] are as before.

Fo[illegible] such slumps, Grilli a[illegible] Watts (200[illegible] performed man 2D[illegible] mulations, using a full nonl[illegible]ear potential fl[illegible]o [illegible] del, and W[illegible] et al. (2005) deri [illegible] a semi-empirical e pressio[illegible] for the minimum su[illegible]e depressi[illegible] η_o computed at $x = x$ [illegible] based on 12 cases of 2D slu[illegible]ps simulations, for [illegible] rious comb[illegible] tions of go erning [illegible] ameters: *B, T, d, θ, γ, Δs,* [illegible] sing an appro ima[illegible] order of [illegible] agnitude alue fo[illegible] e h drod namic coefficien[illegible] C_m = 1,

$$!_o = s_o\left(\frac{T}{B\sin "}\right)\left(\frac{B\sin "}{d}\right)^{[illegible]5}\left(\frac{B}{R}\right)^{0.60}(\Delta\# [illegible] ^{[illegible]39}(\$ - 1)(0.198 - 0.04 [illegible] (\$ - 1)) \qquad \text{(A2.8)}$$

This equ[illegible]tion predicts o er 99[illegible] of the ari[illegible]nce of the computed [illegible] alues of η_o (R^2 = 0.998) an[illegible] is based on the fol[illegible] ing ranges [illegible]f parameter alues [illegible] the computations: $\theta \in [10,30]$ deg., $d/B \in [0.34,0[illegible]]$, $T/b \in [0.1[illegible],0.15]$, $R/b \in [1,2]$, [illegible] $\in [0.1,0.52]$ and $\gamma \in [1.46,2.93]$. As noted b W[illegible]atts et al. (20[illegible]5), o ing to the sim[illegible]ar slide and slump geometr and the identical para[illegible]eterization f[illegible]nd in Eqs. A2.5 and [illegible]2.8 for *T/B* and *d/b*, one can e tend the alidit of [illegible]q. A2.8 to $d/[illegible] \in [0.06,0.5]$, $T/b \in [illegible].10,0.2]$ [Note, Eq. A2.8 has been re-deri ed to pr[illegible] ide higher a[illegible]curac , as compared t[illegible] Eq. (4) in Watts et al. (2005)]. See Fig. A3b for a [illegible]omparison o[illegible] computed alues of η [illegible] to predicted alues from Eq. A2.8, for the 12 comp[illegible]ted slumps.

A.2.3 3D underwater slides [illegible]nd slumps

In parallel ith the 2D slide and slump modeling studies, Grilli et al. (2002) performed a limited number of three-dimensional (3D) of tsunami generated b under ater slides of bulk densit ρ_b in ater of densit ρ_w, on a plane slope of angle θ. These simulations ere later e tended and e perimentall alidated b Enet and Grilli (2003, 2005, 2007) (see also Grilli et al., 2010b). The computational model set-up and parameters for these 3D slides is such as sho n in Fig. A4 and the e perimental set-up is sho n in Fig. A5.

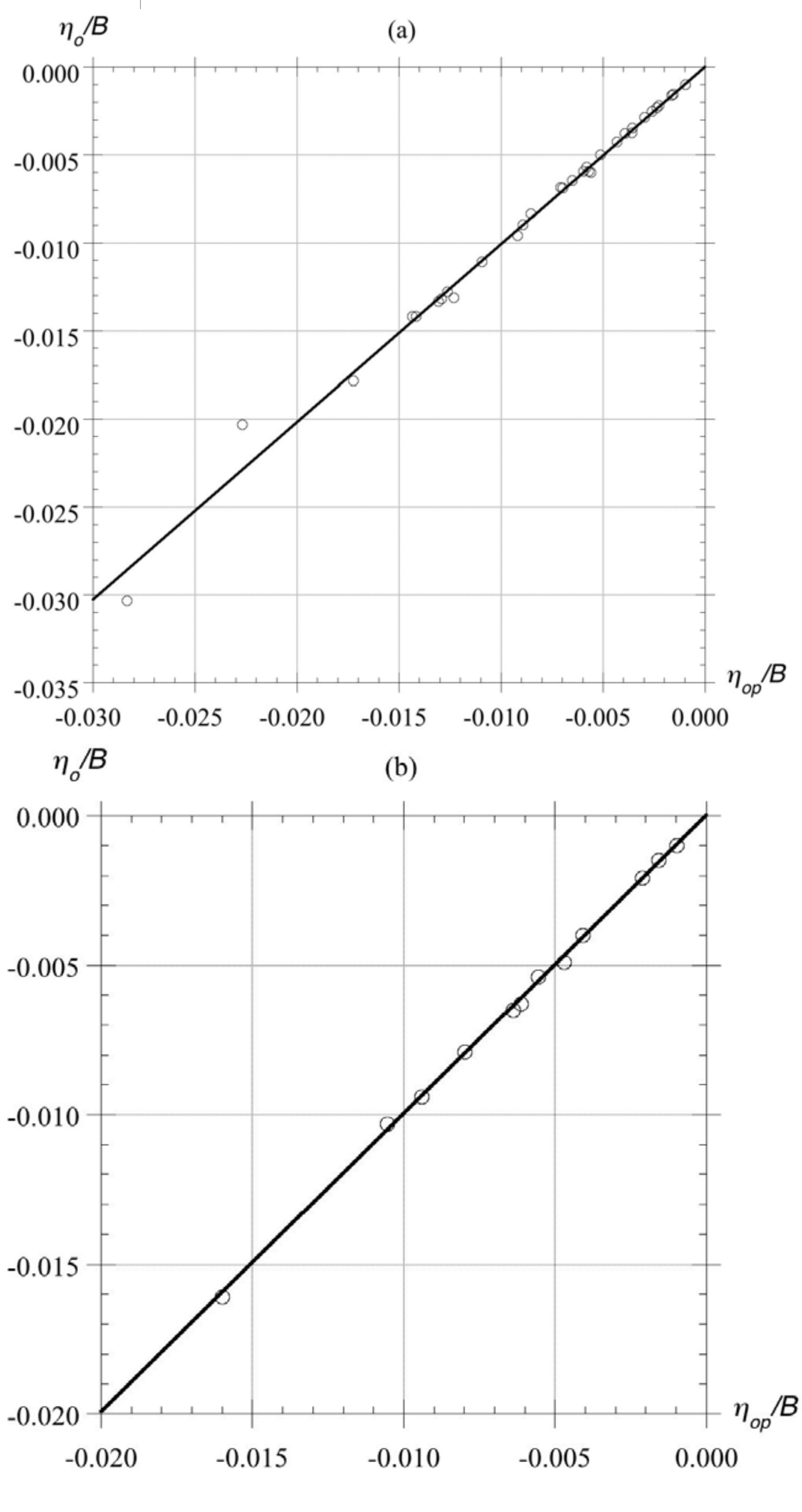

Fig. A3: Comparison of computed η_o ersus predicted η_{op} minimum surface depression at $x = x_o$, for 2D under ater: (a) slides (32) using Eq. A2.5; or (b) slumps (12) using Eq. A2.8.

3D Slide/sl[redacted]sunami so[redacted]rce characteristic amplitude

Although t[redacted]D under a[redacted]ter SMFs that ere numericall modeled a[redacted]ested had a double Gau[redacted]-like geometr , to compare results ith earlier 2D o[redacted]n equi alent semi-ellipso[redacted]slide ha ing the same olume and proportions as the[redacted]inal slide is calculated, [redacted]length *B,* thickness *T,* and idth *W*. The ater depth [redacted]e the initial location, *x* [redacted]of slide ma imum thickness is again defined as *d*.

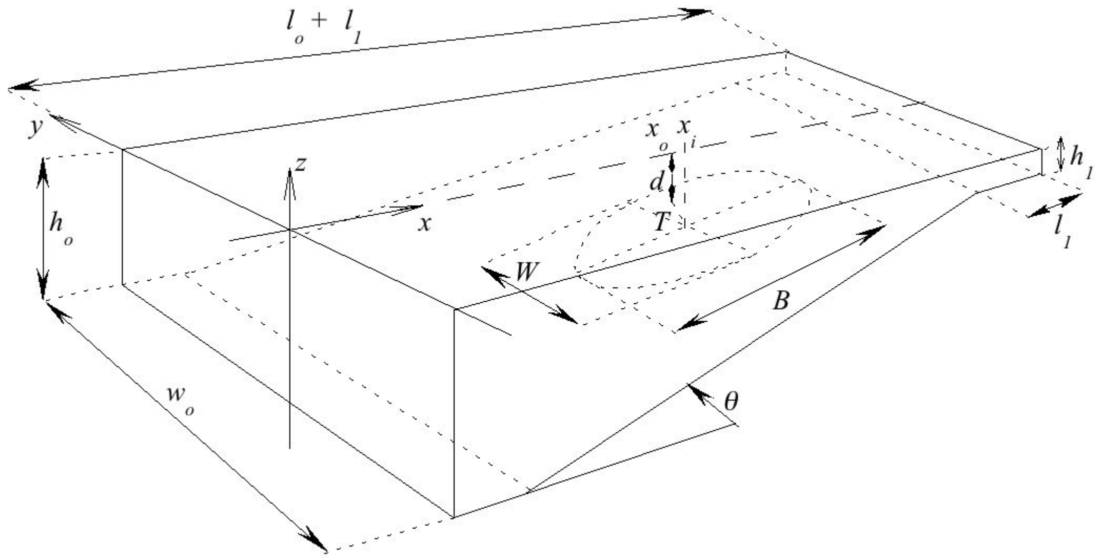

Fig. A4[redacted]arameters definition for 3D slide computations (from Grill[redacted]t al., 2002).

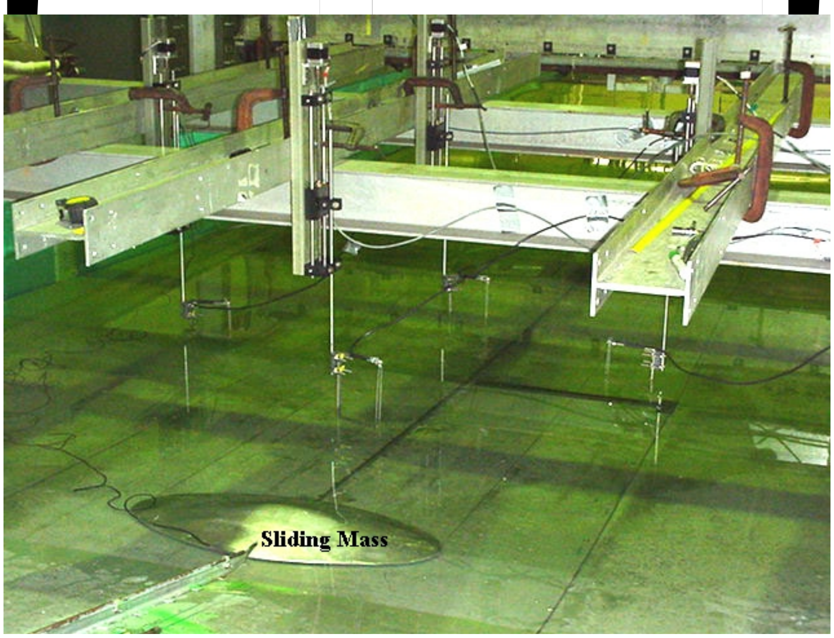

Fig. A5: E perimental set-up for Enet and Grilli's (2003, 2005, 2007) e periments for a rigind 3D slide of Gaussian shape (ith elliptical footprint) sliding do n a 15 deg. plane slope for a ariet of initial submergence *d*.

T D slide olume nd main cross-sectio thus found for semi-ellipsoid as,

$$V_s = \frac{}{} WBT \quad \text{with} \quad A_s = \frac{\pi}{4} WT \tag{A2.9}$$

a slide mo ion is a ain modeled ith equ s A2.3 and A2.

Grill et al. (2002), Enet and Gril 005) and Grill al. (2010b) simulated s ace ele ations generated b 3D slides a found that the all qualitati el similar t ose sho n in Fig. A6, hich correspon o a rigid slide (aussian shape) mo ing d n a θ = 15 deg. slope, ith an initial su ergence d = 0.12 m (x_o = 0.764, from Eq. A 1). The sub-figures A6 correspond to e: $t = t_o/4$; (b) 2; (c) $3t_o/4$; and (d) t_o (tical scale is e aggerated), ith oth parameters bei identical to those of l orator e periments b Enet and Grill 007). Their lab tor model slide had a s cific densit γ = 2.435 and a Gaussian s e ith dimensio ($b(\varepsilon)$ = 0.395, w = 0.68, T 0.082) m (see Figs. A2, A5), but appl Grilli and Enet's ansformation equations, find the dimensions (B, W, T) of an equ lent semi-ellipso slide, ith same olume a proportion as the Gaussian shape slid i.e., $b/B = w/W$, g. A4). These equations a o allo finding the relationship bet een e kinematics of th 3D Gaussian shape slide o Enet and Grilli (2007) and that of the equ alent semi-ellipso d, i.e.,

$$a_o = g \quad \theta\left(\frac{\gamma -}{\gamma + C_m}\right) \qquad u_t = \left(gB \quad \frac{\gamma -}{C_d^{'}}\right)^{-} \qquad C_d = C_d \sqrt{\frac{\chi - \varepsilon}{\pi \quad - \varepsilon \quad \chi \quad - \varepsilon}}$$

$$C = \operatorname{acosh}\left(\frac{1}{\varepsilon}\right) \; ; \; \chi = \frac{2}{C} \operatorname{atan}\sqrt{\frac{1-\varepsilon}{1+\varepsilon}} \quad B = b\sqrt{\frac{6}{\pi}\frac{\chi^2 - \varepsilon}{1-\varepsilon}} \quad \text{and} \quad W = \frac{B}{b} w \tag{A2.10}$$

here C_m and C_d are h drod namic coeffi ents found b cur e fitting the measured 3D Gaussian slide motion using the slide kinematics equations (Eqs. 9 and 10 in Enet and Grilli, 2007). Note that if one uses the ear ier formulation of the slide kinematics A2.4, the drag coefficient is: $C''_d = (3\pi/8)\, C'_d$. Also note that, in the absence of such detailed e perimental measurements, these coefficients had been appro imated to $C_m = C_d = 1$ in the earlier ork of Grilli and Watts (2005) and Watts et al. (2005) for 2D SMFs.

Thus, for the equi alent 3D semi-ellipsoid slide kinematics, described b Eqs. A2.10, e find that the added mass coefficient does not change as compared to the original slide, but the iscous drag coefficient C'_d depends on slide shape, hich is parameterized as ele ation ζ (Fig. A2), in a es (ξ, ν) b coefficient ε as,

$$\zeta(\xi,\nu) = \frac{T}{1-\varepsilon}\left\{\operatorname{sech}\left(\frac{2C\xi}{b}\right)\operatorname{sech}\left(\frac{2C\nu}{w}\right) - \varepsilon\right\} \tag{A2.11}$$

For their e perimenta Enet nd Gri (20 ported $\varepsilon = 0.717$, hich ields using Eq. A2.10: C 2, $\chi =$).895, $'_d =$ C_d (and $C''_d = 1.251C_d$), and dimensions: $B = 0.29$ = 0.08 m, W = 0.5 for the semi-ellipsoid. No , for the case of Fig. A6, = 0.12 n, e f d C_m 685 and $C_d = 0.332$ in Enet and Grilli's (2007) Table match he e p rimen measured slide motion. Hence, appl ing Eqs. A2.3 an 0, e fi d $t_o =$ 74 s a = 3.52 m.

To compare th erimentall mea ured l surface depressions, referred to as the tsunami source cteristic amplit de, to e predicted in computations, one can of course perform nonlinear 3D omput s, such as sho n in Fig. A5, for each specific case. Do , Enet and Grill (2005 07) and Grilli et al. (2010b) found a er good agreeme t een e perim ntal a omputed surface ele ations at a number of gages, as a ion of time. Ho e er, use of the high computational cost of such 3D simulation as done for 2D SMFs, desirable to deri e semi-empirical equations that can b d to quickl d fine la lide tsunami source ele ation in practical situations, a unction of a fe go e g parameters. Watts et al. (2005) alread attempted to so b obser ing, ba on the limited number of 3D computations of Gril al. (2002), that the in surface depression in 3D, η_o^{3D}, decreased as a functio he ratio of the character tsunami a elength λ_o (Grilli and Watts, 1999, 2005) to MF idth, appro imate s,

$$\eta_o^{D} \cong \eta_o \frac{\quad}{+\frac{\lambda_o}{W}} \qquad \lambda_o = t_o\sqrt{gd} \qquad \text{(A2.12)}$$

here η_o is the 2D ch teristic amplitude gi en equations A2.5 and A2.8, for slides or slumps. Enet and lli (2007) applied this e tion to the original semi-empirical equations deri ed b tts et al. (2005) for 2D s des, and reported a good agreement ith their measureme of η_o^{3D}.

Here, as a ali tion of the proposed equa ons for TOPICS, e ha e combined the impro ed formulati n of the 2D characteristic mplitude gi en b Eq. A2.5 and re-deri ed a best fit for q. A2.12 for the lateral D spreading effect, b appl ing the equations to all the e erimental cases of Enet a d Grilli (Table 1), for non-breaking a es, hich correspo d to submergences: $d = 0.$ 61 – 0.189 m. In each case, e used the reported alues of C_n, hich range from 0.582 0.767 (mean 0.637, st.d. 0.067), and C_d, hich range from 0 302 to 0.509 (mean 0.386, .d. 0.076). This ields,

$$\eta_o^{3D} = \eta_o \frac{0.935}{\left(1+\frac{\lambda_o}{W}\right)^{0.872}} \quad \text{or} \quad \eta_o^{3D} = \eta_o 0.535 e^{-0.211\frac{\lambda_o}{W}} \quad \text{with} \quad \lambda_o = t_o\sqrt{gd} \qquad \text{(A2.13)}$$

ith the second formulation pro iding a slightl better fit, hen combined ith Eq. A2.5 than the first one, and e plaining o er 96% of the e perimental ariance ($R^2 = 0.961$).

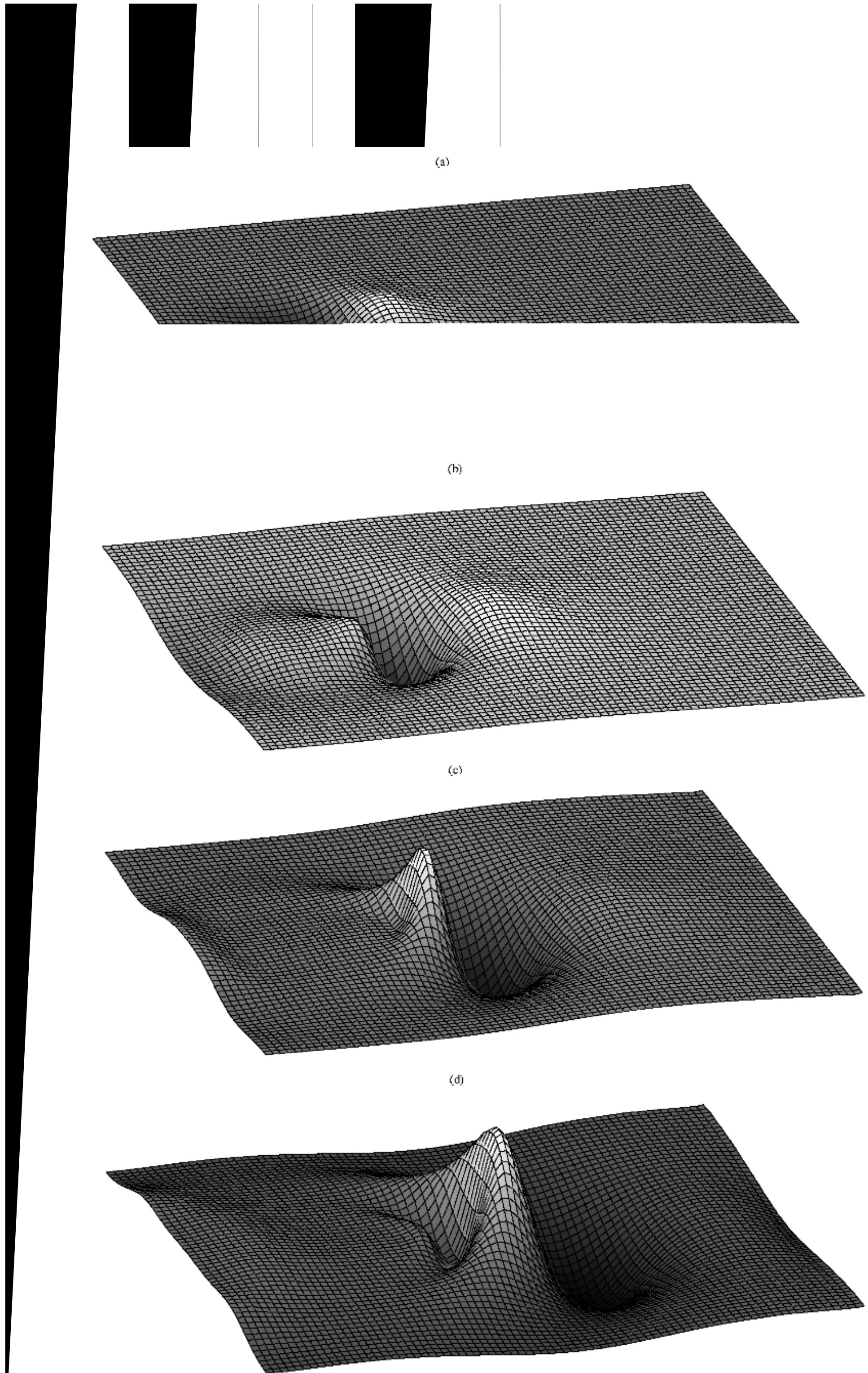

Fig. A6: E ample of free surface ele ation computed for a 3D SMF, sliding o er a $\theta = 15$ deg. slope, at time $t = t_o/4$; (b) $t_o/2$; (c) $3t_o/4$; and (d) t_o (ertical scale is e aggerated). The slide equi alent semi-ellipsoid has dimensions : $B = 0.298$ m, $T = 0.082$ m, $W = 0.515$ m, ith $\gamma = 2.435$ and an initial slide submergence $d = 0.120$ m ($x_o = 0.764$, from Eq. A2.1), for hich $t_o = 1.74$ s based on Eqs. A2.3 and A2.4, using $C_m = 0.685$ and $C_d = 0.416$ to match e perimentall measured slide motion (results based on Enet and Grilli, 2005, 2007; Grilli et al., 2010b).

B contrast, [illegible]ing Watts et al. equations as summ[illegible]zed in Gr[illegible]nd Enet (2007), hich include Eq. [illegible].12, one can e plain o er 95% of t[illegible]e perim[illegible] ariance (R^2 = 0.955). Fig. A6 sho[illegible] the comparison of measured and [illegible]dicted *3*[illegible]*racteristic amplitudes* (i.e., surface[illegible]epression at $x = x_o$), based on the [illegible]ter formu[illegible] and on the ne one, combining E[illegible] A2.12 ith the second Eq. A2.13. T[illegible]e graphic[illegible]reement is quite good.

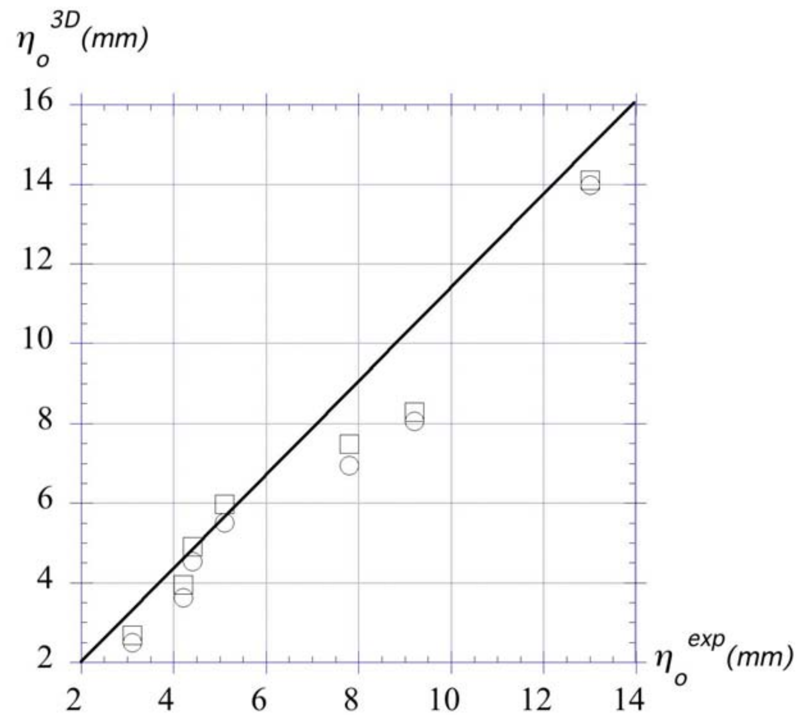

Fig. A7: E periments of Fig. A5. Prediction of e perimental[illegible] measured characteristic tsunami depressions η_o^{exp} using : (☐) the initial parameteriza[illegible]on of Watts et al. (2005) (R^2 = 0.955); (o) the ne l proposed parameterization using E[illegible]s. A2.5 and 2nd Eq. A2.13 (R^2 = 0.961).

3D Slide/slump tsunami source elevation

In 3D, as can be seen in Fig. A6, the free surface sho s an [illegible]itial depression abo e the slide initial location, ith a smaller a e of ele ation ahead [illegible]f it (a); then the 3D a e propagation graduall spreads out these features both for [illegible]ard and laterall , as time increases (b-d); this lateral spreading has a shape similar t[illegible] a Gaussian-like sech^{2}(κ) function. A second, crescent shape, ele ation a e then g[illegible]raduall gro s behind the initial depression and propagates both offshore and onshore ([illegible]he latter causing runup). In the median ertical plane y = 0, the surface ele ation appears qualitati el similar for small time $t < t_o$ to that computed for 2D slides (e.g., Grilli and Watts's (2005) Figs. 11 and 12). As as found b Grilli and Watts (2005) in 2D, ma imum tsunami generation, defined b the deepest surface depression abo e the slide instantaneous location, η_{min}, is reached for $t \approx t_o$ (e.g., Fig. A5d), at hich time Eq. A2.3 ields a slide displacement: s_{min} = 0.4338 s_o (s_{min} =1.76 m for the case of Fig. A6, or x_{min} =2.24 m; Eq. A2.1). Additionall , the same ork sho ed that the 2D characteristic tsunami amplitude η_o is rea ed for all sub ergenc depths *d,* the anal zed, at $t \approx 0.5t_o$ (e.g., Fig. A5b). Finall , in e 2D slides studied b Grilli and Watts (2005) the found across all initial sub ergences,

$$\eta_{min} \approx (2\text{-}2.5)\ \eta_o \tag{A2.14}$$

Although a similar thorough computational stud of 3D slides as not performed b Grilli et al. (2002) and Enet and Grilli (2003, 2005), due to the high computational cos s at the time, similar obser ations ere made for 3D slides, at least qualitati el . Th s, in their laborator e periments for 3D rigid slides, Enet and Grilli (2003, 2005) fou d that the ma imum depression η_o abo e at $x = x_o$ occurred in the arious tested sub ergences, for $t \approx 0.25\text{-}0.35t_o$ (i.e., slightl earlier than for 2D slides; their Fig. 14) and ith a significantl reduced alue, as compared to 2D slides, as a result of 3D a e ene g radiation from the initial slide location, as alread quantified b Eqs. A2.12 and A2.13.

In ie of these salient features of the initial free surface ele ation generated b 3D SMFs, and to a oid performing full computations of such 3D tsunami sources, each time this is required to simulate a SMF tsunami in practical situations, Watts and Grilli (2005) proposed a parameterization of the initial tsunami ele ation at the time of ma imum surface depression $t = t_o$, $\eta(x,y)$ and horizontal (depth-a eraged) elocit $\mathbf{u}(x,y)$, to be used as an initial condition in 2D horizontal long a e tsunami propagation models such as FUNWAVE. This parameterization as built around the ork of Grilli and Watts (2005), Grilli et al. (2002), and Enet and Grilli (2003, 2005), and uses 2D characteristic amplitude Eqs. A2.5 and A2.8, for slides and slumps, Eqs. A2.12 for the lateral 3D spreading, and other considerations discussed belo .

Specificall , in the original TOPICS implementation of Watts et al.'s (2005) parameterization for slides or slumps the surface ele ation of the tsunami source as modeled as the sum of t o Gaussian functions of x (g_1 and g_2) multiplied b a sech^2 function of y. Ho e er, in ie of the arious ne parameterizations proposed, coefficients α_1 and α_2 ere added, in order for $\eta_{2D}(x,y)$ to be nearl η_{min} at $x = x_{min}$ and η_{max} at $x = x_{max}$, for $y = 0$, as,

$$\begin{aligned}
&\eta_{3D}(x,y,t_o) = \eta_{\min} f\left(W\right) \operatorname{sech}^2\left(\kappa f\left(W\right)\frac{y}{W}\right)\left\{\alpha_1 g_1(x) - \alpha_2 \kappa' g_2(x)\right\} \\
&g_1(x) = \mathrm{e}^{-\left(\frac{x - x_{\min}}{\kappa' \lambda_o}\right)^2} \;;\; g_2(x) = \mathrm{e}^{-\left(\frac{x - x_{\min} - \Delta x}{\lambda_o}\right)^2} \\
&\alpha_1 = \frac{1 + \kappa' g_2(x_{\min})}{1 - g_1(x_{\max}) g_2(x_{\min})} \quad ; \quad ; \alpha_2 = \frac{1 + (1/\kappa') g_1(x_{\max})}{1 - g_1(x_{\max}) g_2(x_{\min})}
\end{aligned} \tag{A2.15}$$

 ith, in the earlier TOPICS parameterization,

$$x_{\min} = \Delta x_o - \ x_o \quad ; \quad \Delta x_o = c_o (x_o + c_1 s_o \cos\theta) \quad ; \quad x_{\max} = x_{\min} + \Delta x$$

$$\Delta x = c_2 \lambda_o \quad ; \quad \ldots = -f_1 \eta_o \quad ; \quad \eta_{\max} = f_2 \eta_o \quad ; \quad \kappa' = f_2 / f_1$$

$$f(W) = 1 - \exp\left\{ \ldots \frac{W}{\lambda_o}\left(1 + c_4 \frac{W}{\lambda_o}\right)\right\} \quad ; \quad \kappa = 3 \qquad \text{(A2.16)}$$

… c_3 = 2.091 and c_4 … .090 and η_o denoting the 2D characteristic amplitude.

Additionall , fo … ides, e ha e,

$$c_o = 0.95 \quad ; \quad c \ldots \log(\cosh(1)) = 0.4338 \quad ; \quad c_2 = 0.5$$

$$f_1 = 2.52 \quad ; \quad f \ldots 0.512\left(1 + 0.25 \frac{d}{d_{ref}}\right) \quad ; \quad d_{ref} = B \sin\theta \qquad \text{(A2.17)}$$

a … d for slumps,

$$c_o = 0.565 \quad ; \quad \ldots = 1 - \cos(1) = 0.4597 \quad ; \quad c_2 = 0.8 \quad ; \quad S_g = \frac{s_o \sin\theta}{d} = \frac{s_o}{B}\frac{d_{ref}}{d}$$

$$f_1 = 3.479\left(\frac{1 - 1 \ldots 02 S_g + 1.865 S_g^2}{\ldots + 3.168 S_g}\right) \quad ; \quad f_2 = 2.057\left(\frac{1 - 0.599 S_g + 1.096 S_g^2}{1 + 2.932 S_g}\right) \qquad \text{(A2.18)}$$

here S_g denotes the so-called submergence number.

The lateral spreading function $f(W)$ in Eqs. A2.15 and A2.16, although of the same nature, is different from those proposed earlier in Eq. A2.13, on the basis of the e perimental alidation. This function as ell as the sech^2 function in Eq. A2.15, ere parameterized initiall in TOPICS, based on Grilli et al.'s (2002) 3D numerical simulations (such as sho n in Fig. A6).

In ie of the e perimental alidation presented abo e, e no use in Eq. A2.15, the ne parameterization of the lateral spreading function, corresponding to the second Eq. A2.13, as,

$$f(W) = 0.535 \exp\left\{-0.211 \frac{\lambda_o}{W}\right\} \quad \text{with} \quad \kappa = 6 \qquad \text{(A2.19)}$$

Using Eq. A2.19 to calculate the reduction of 2D characteristic ele ations in Eq. A2.15, instead of the earlier parameterization of lateral spreading, e also find that, in order for most of the lateral damping of the 3D surface ele ation to occur o er four times the idth of the slide (i.e., $4W$), in the sech^2 function of y, as as specified in earlier parameterizations based on Grilli et al.'s 3D computations, one no needs to use a ne alue of κ = 6, as indicated in Eq. A2.19.

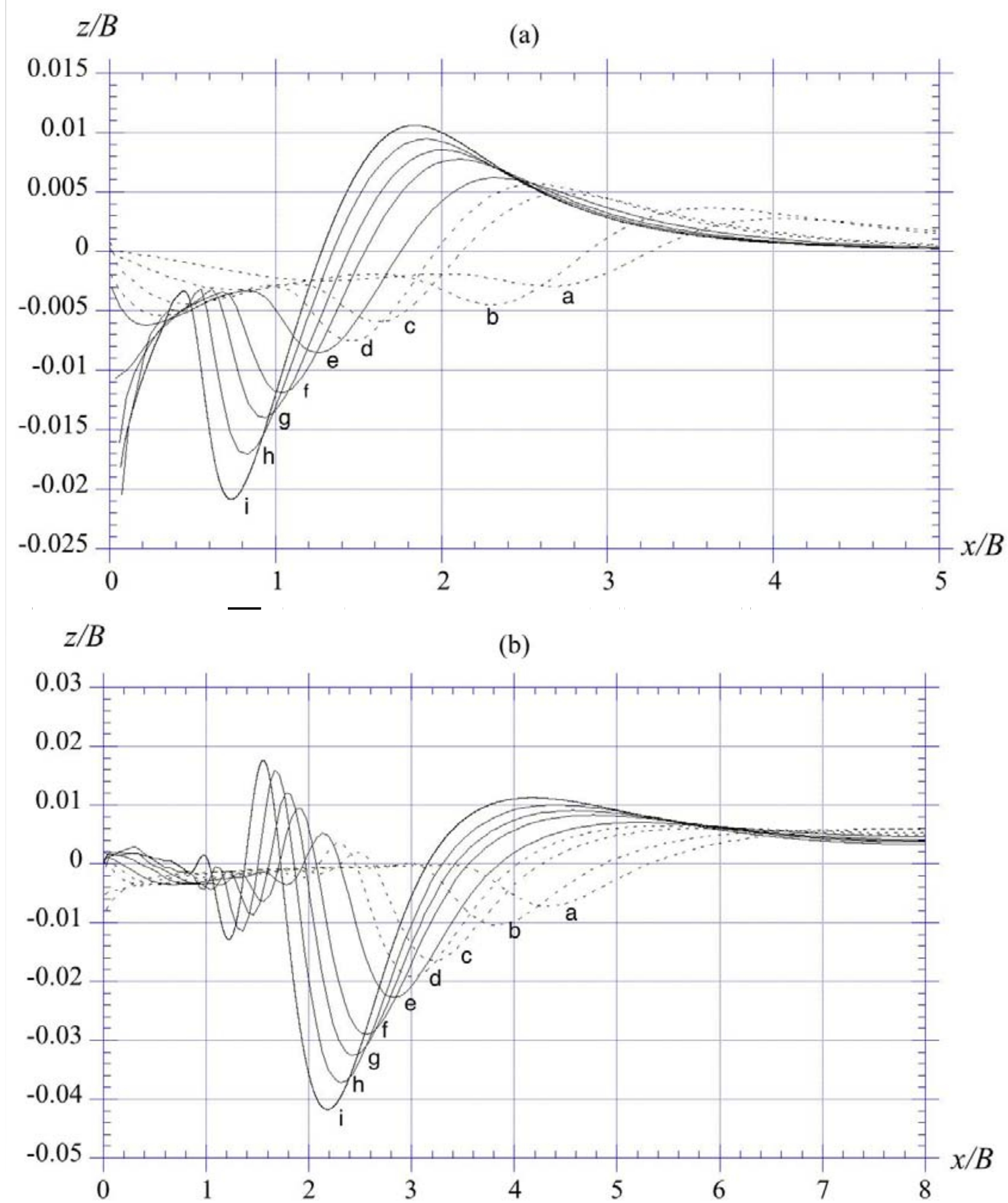

Fig. A8: 2D computations of semi-elliptical under ater slide b Grilli and Watts (2005) (ith $\theta = 15$ deg., B = 1 m, T = 0.052 m, $\gamma = 1.85$, $C_m = C_d = 1$), for initial depth d = a: 0.625; b: 0.5; c: 0.35; d: 0.3; e: 0.259; f: 0.2; g: 0.175; h: 0.15 m, at time: (a) hen the ma imum depression η_o is reached at $x = x_o$; (b) $t = t_o$.

The rest of Eq. A2.15, hich is function of x, as initiall parameterized based on 2D numerical simulations (e.g., Fig. 11 in Grilli and Watts, 2005). A more careful re-anal sis of the latter computations is done in the follo ing, for a $\theta = 15$ deg. slope, and a 2D semi-elliptical slide ith B = 1 m, T = 0.052 m, and $\gamma = 1.85$. Using $C_m = C_d = 1$, Eqs. A2.3 and A2.4 ield s_o = 4.477 m and t_o = 2.432 s. Initial submergence is aried ithi[illegible] 0[illegible] 0.[illegible]n (9 depth alues); for each of tho[illegible]q. A2.1 ields x_o. Grilli and V[illegible] g[illegible]om[illegible]l free surface profiles as a functio[illegible]f time, hich are partl sho[illegible] Fi[illegible]a,b[illegible](a) the (different) times hen the m[illegible]mum surface depression η_o is [illegible]he[illegible] = [illegible]nd (b) at time $t = t_o$, hen the abs[illegible]e free surface minimum η_{min} i[illegible]ch[illegible]e [illegible]e fits ere calculated on the basis o[illegible]se results, as (Fig. A9),

$$\eta_{\min} [illegible] \eta_o [illegible] = 1.10\left\{1 + 2.21\frac{d}{d_{ref}}\left(1 - 0.314\frac{d}{d_{ref}}\right)\right\} \quad \text{(A2.20)}$$

$$[illegible]_{\max} [illegible] \eta_o [illegible] = 0.347\left\{1 + 1.06\frac{d}{d_{ref}}\left(1 + 0.409\frac{d}{d_{ref}}\right)\right\} \quad \text{(A2.21)}$$

ith R[illegible] = 0.[illegible] and [illegible]99, respecti el .

[illegible]D er[illegible] 9 de[illegible] alues, the a erage alue of f_1 is 2.6[illegible] hich is quite close to the 2.52 [illegible]ue u[illegible] earli[illegible]n Eq. A2.17. Based on these results, [illegible]e also deri e the follo ing cur e[illegible]ts (F[illegible]A10),

$$x_{\min} [illegible] x_o - [illegible] \; ; \quad \Delta x_o = c_o(x_o + c_1 s_o \cos\theta) \; ; \quad c_o = 2.[illegible]43 \; ; \quad c_1 = 0.124 \quad \text{(A2.22)}$$

$$x_{\max} [illegible] x_{\min} + \Delta[illegible] \; ; \quad \frac{\Delta x}{B} = c_{21}\left(1 - c_{22}\frac{\lambda_o}{B}(1 - c_{23}\frac{\lambda_o}{B})\right) \; ; \quad c_{21} = [illegible]96 \; ; \; [illegible] = 0.270 \; ; \; c_{23} = 0.211 \quad \text{(A2.23)}$$

ith R^2 = [illegible]998 an[illegible] 0.996, respecti el . These are quite different from the earlier parameteriza[illegible]on for[illegible]lides used in Eqs. A2.16, A2.17. Fig. A9 sho s the relationship bet een x_{min}[illegible] x_{max}, a[illegible]d x_o, hich here, for constant slide thickness T and slope angle θ is linear rela[illegible]d to d [illegible]r d/d_{ref} (Eq. A2.1). Moreo er, from Eq. A2.13, e see that, in the present case, λ_o is si[illegible]pl proportional to $d^{1/2}$, hich further e plains the good linear fit of x_{max} ith x_o.

We [illegible]ee in F[illegible]g. A8b that the free surface at $t = t_o$ can indeed essentiall be appro imated b the sum of t o Gaussian functions, respecti el centered on the location of [illegible]inimum depression $x = x_{min}$ (negati el) and on that of the first ele ation a e do nstream of it, defined as $x = x_{max} = x_{min} + \Delta x$ (positi el); this confirms the parameterization introduced in Eq. A2.15. Also note in Fig. A8b, the second ele ation a e, hich follo s (upstream) the depression a e at x_{min} (as also seen in Fig. A6d), and is neglected in the parameterization A2.15. One of the reasons for this (besides reducing the comple it of the parameterized source geometr) is that, in numerical or laborator e periments discussed so far, the entire seafloor as modeled as a surface piercing plane of constant slope, hich is likel to significantl enhance this second "rebound" surface ele ation a e. In natural shel es, b contrast, for SMFs occurring on the continental shelf slope, this rapid reflection and enhancement do not occur on the

[redacted]

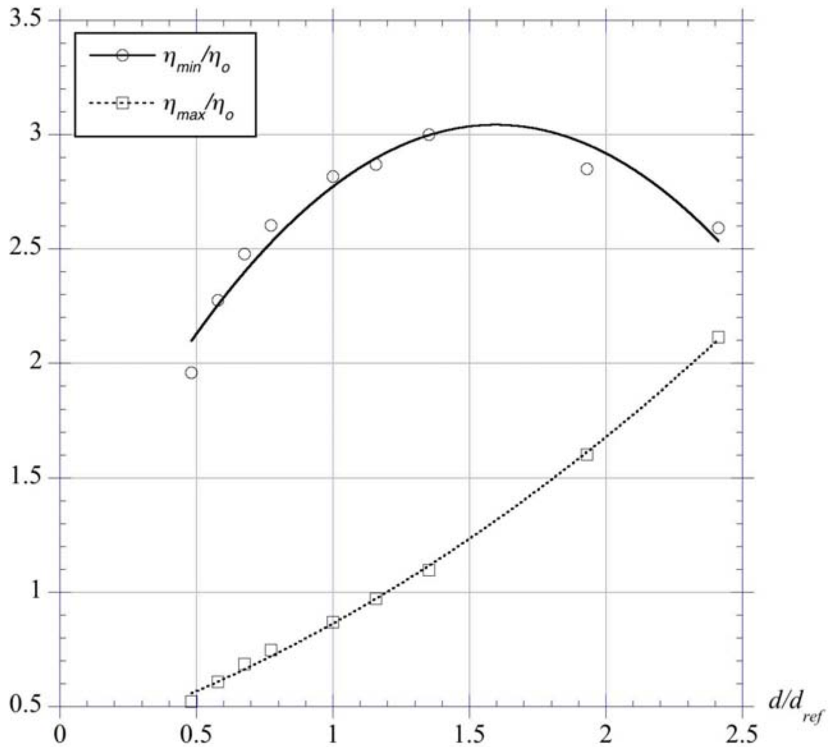

Fig. A9: Data and cur e fit based on Grilli an[redacted]atts’ (2005) computations of Fig. A8, for minimum and ma imum[redacted]D surface ele ations.

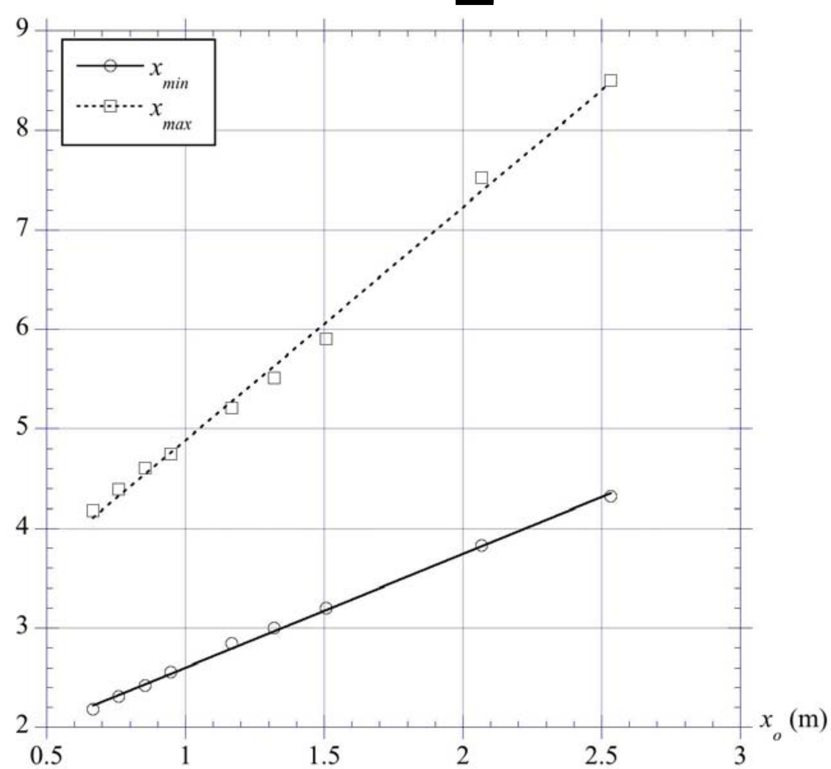

Fig. A10: Data and cur e fit based on Grilli and Watts’ (2005) computations of Fig. A8, for x location of minimum and ma imum 2D surface ele ations.

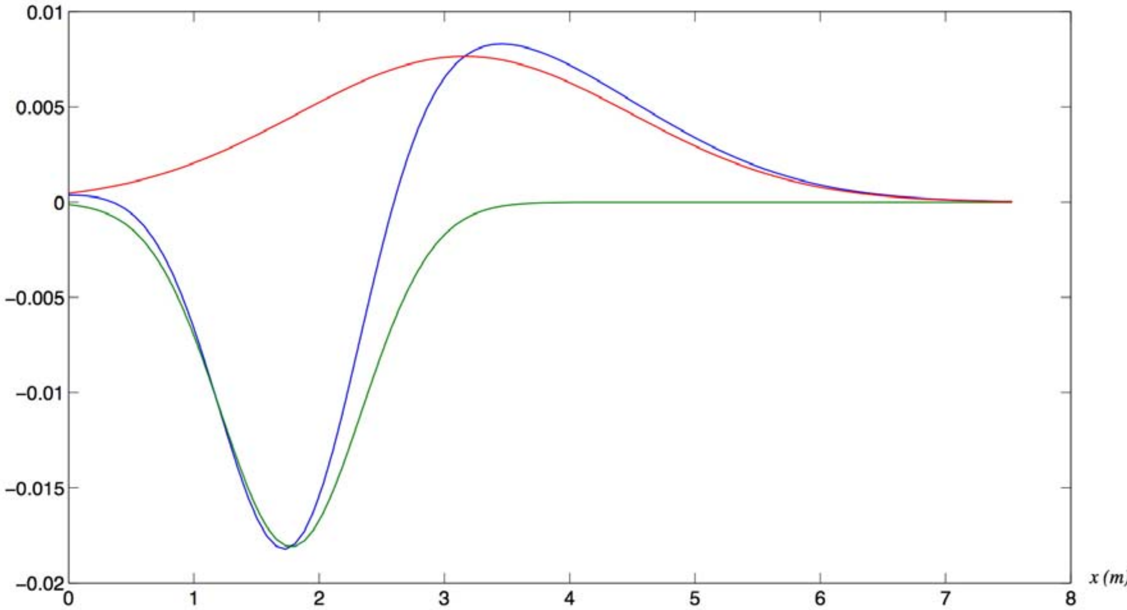

Fig. A11: Free surface elevation $\eta(x,0)$ for $y = 0$, at t_o, (blue line) in empirical tsunami source elevation Eq. A2.15, with parameterization of Eqs. A2.5 and A2.19-A2.23, for the case of Fig. A6 ($\theta = 15$ deg., $B = 0.298$ m, $T = 0.082$ m, $W = 0.515$ m, $\gamma = 2.435$, $d = 0.120$ m), for which $x_o = 0.764$ m, $t_o = 1.74$ s and $s_o = 3.52$ m, using $C_m = 0.685$ and $C_d = 0.416$. The red and green lines show the two Gaussian functions of x in Eq. A2.15.

onshore side, due to the continental shelf over which the second "rebound" wave can spread out.

Using Eq. A2.15 with the parameterization in Eqs. A2.19-A2.23, we now calculate the 3D free surface elevation (i.e., SMF tsunami source) for the case computed in Fig. A6, which corresponds to one of Grilli and Enet's (2007) experiment for a $\theta = 15$ deg. plane slope, and a 3D Gaussian-shape slide with dimensions of the equivalent semi-ellipsoid: $B = 0.298$ m, $T = 0.082$ m, $W = 0.515$ m (Eqs. A2.10), density $\gamma = 2.435$ and an initial slide submergence $d = 0.120$ m (for which $x_o = 0.764$ m, $t_o = 1.74$ s and $s_o = 3.52$ m), using $C_m = 0.685$ and $C_d = 0.416$. For this case, Eqs. A2.5 and A2.19-A2.23 yield: $\eta_o = 0.0242$ m, $\eta_o^{3D} = 0.0060$ m ($\eta_{o,exp}^{3D} = 0.0051$ m), $f(W) = 0.247$, $\eta_{min} = -0.0181$ m ($f_1 = 3.03$), $\eta_{max} = 0.0077$ m ($f_2 = 1.28$), $\kappa' = 0.422$, $x_{min} = 1.777$ m, $x_{max} = 3.160$ m, $\Delta x = 1.383$ m, $\lambda_o = 1.883$ m, and $\Delta x / \lambda_o = 0.734$. For this case, Fig. A11 shows a cross section in free surface elevation: $\eta(x,0)$ for $y = 0$ (blue line), with the two Gaussians of Eq. A2.15 shown (in green and red). We see that the surface elevation at $y = 0$ takes the expected η_{min}, x_{min}, η_{max}, and x_{max} values.

Fig. A12 then shows the full 3D source elevation (i.e., $\eta(x,y)$ at t_o), predicted for this case by Eq. A2.15, which is to be compared with computations of Fig. A6. While the agreement with Fig. A6b (at $t = t_o/2$) appears qualitatively good, due to the appearance of the second (rebound) elevation wave in computations for later time (see above discussion), hich is not included in the semi-empirical free surface ele ation, the qualitati e agreement is less good for Fig. A6d, hich is at $t = t_o$, at the time of ma imum tsunami generation. Ho e er, despite these differences in shape, the empirical solution has a good agreement (not sho n here), on the minimum surface depression and ma imum ele ation, as ell as their location, ith respect to the starting location of the slide, and good agreement on a elength (in x direction) and lateral spreading.

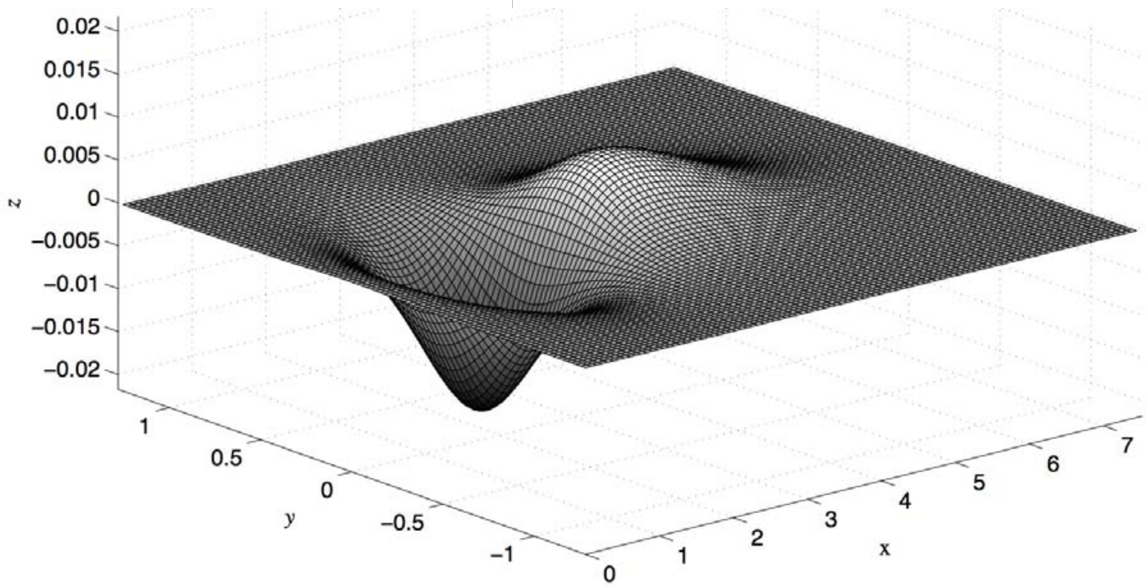

Fig. A12: Free surface ele ation $\eta(x,y)$ at t_o, i.e., SMF tsunami source, from empirical tsunami source ele ation Eq. A2.15, ith parameterization of Eqs. A2.5 and A2.19-A2.23, for the case of Fig. A6, A11.

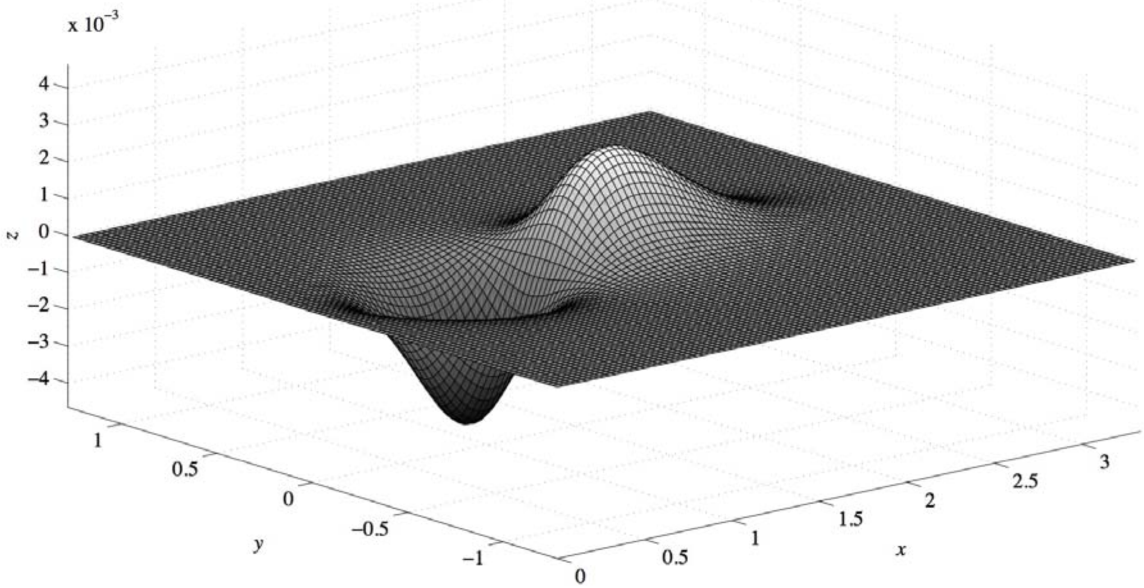

Fig. A12: Free surface ele ation $\eta(x,y)$ at t_o, i.e., SMF tsunami source, from empirical tsunami source ele ation Eq. A2.15, ith parameterization of Eqs. A2.5 and A2.19-A2.23, for the case of Fig. A6, A11.

Since free surface ele ations features at time t_o appear qualitati el similar in computations for slide or slumps (e.g., Grilli et al., 2002; Grilli and Watts, 2005), the same parameterization of the initial source ele ation as for *slides* (described b Eq. A2.15, ith η_o calculated b Eqs. A2.6-A2.8), is used for *slumps* as ell. For the lateral spreading function *f(W)*, e use the ne parameterization of Eq. A2.19. For the other parameters, e use the slump parameterization A2.18, hich as more recentl done in TOPICS and alidated on a number of case studies (e.g., Tappin et al., 2008).

Fig. A.12, for instance sho s the initial free surface calculated this a for a slump of geometr similar to the earlier slide, i.e., for the equi alent semi-ellipsoid: B = 0.298 m, T = 0.082 m, W = 0.515 m (Eqs. A2.10), densit γ = 2.435 and an initial slide submergence d = 0.120 m on a 15 deg. slope (for hich x_o = 0.764 m). Using C_m = 0.685, $\Delta\phi$ = 20 deg. and a short slump displacement on the slope, $\Delta s = 2B$ =0.496 m, Eqs. A2.6-A2.8 ield, R = 1.707 m, t_o = 615 s, s_o = 0.248 m, η_o = 0.0078 m, η_o^{3D} = 0.0032 m, $f(W)$ = 0.407, η_{min} = -0.0039 m (f_1 = 1.22), η_{max} = 0.0024 m (f_2 = 0.76), x_{min} =0.951 m, x_{max} =11.551 m, λ_o = 0.667 m.

3D Slide/slump tsunami source initial flow velocity

Initial elocit $\mathbf{u}(x,y)$ is specified for the semi-empirical 3D tsunami source ele ations, on the basis of (depth-integrated) mass conser ation for long a es. For linear long a es of celerit $c = (gh)^{1/2}$, one can sho (e.g., Grilli, 1997), that in the direction of propagation, $|\mathbf{u}| \approx c\eta$, here $\eta(x,y)$ is the local free surface ele ation. In the present case, one can estimate the local direction of propagation as the free surface steepest decent, $\mathbf{d} = \nabla\eta / |\nabla\eta|$.

6. REFERENCES

Abadie, S., C. Gandon, S.T. [illegible]li, R. Fabre, J. Riss, E. Tric, D. Morichon, and S. Glockner. 2009. 3D nu[illegible]rical simulations of a es generated b subaerial mass failures. Application to[illegible] Palma case. In *Proc. 31st Intl. Coastal Engng. Conf.* (J. McKee Smith, ed.) [illegible]CE08, Hamburg, German , Sept. 2008), pp. 1384—1395. World Scientific [illegible]blishing Co. Pte. Co.

Abadie, S., D. Morichon, S. G[illegible]li, and S. Glockner. 2010. Numerical simulation of a es generated b la[illegible]slides using a multiple-fluid Na ier-Stokes model. *Coastal Engng.* 57: 779[illegible]794.

Abadie, S., J. Harris, and Grilli[illegible].T. 2011. Numerical simulation of tsunami generation b the potential flank [illegible]llapse of the Cumbre Vieja Volcano. In *Proc. 21st Offshore and Polar Eng[illegible]g. Conf.* (ISOPE11, Maui, HI, June 19-25, 2011), Intl. Society of Offshore and [illegible]olar Engng.

Andrade, C., P. Borges, and [illegible].C. Freitas. 2006. Historical tsunami in the Azores archipelago (Portugal). *[illegible]ournal of Volcanology and Geothermal Research*. 156: 172–185.

Argus, D. F., R. G. Gordon, C[illegible] DeMets, and S. Stein. 1989. Closure of the Africa-Eurasia-North America[illegible]late motion circuit and tectonics of the Gloria fault. *J. Geophys. Res.* 94: 5585[illegible]—5602.

Baptista, M. A., and C. Lemo[illegible]. 2000. The source of the 1722 Algar e earthquake, inferred from h drod [illegible]amic modeling of the associated tsunami. *European Geophysical Society, 25[illegible] general assembly*. Nice, France, April 25-29, 2000.

Barkan, R., U. S. ten Brink, an[illegible] J. Lin. 2009. Far field tsunami simulations of the 1755 Lisbon earthquake: Imp[illegible]ications for tsunami hazard to the U.S. East Coast and the Caribbean. *Marine Ge[illegible]logy*. 264: 109-122.

Bent, A. L. 1994. *Seismogra[illegible]ms for historic Canadian earthquakes: The 19 November 1929 Grand Banks earthquake*. Geological Sur e of Canada, Open File Report 2563. 36 pp.

Bent, A. L. 1995. A comple double-couple source mechanism for the Ms 7.2 1929 Grand Banks earthquake. *Bulletin of the Seismological Society of America*. 85: 1003—1020.

Br ant, E. 2001. *Tsunami – the underrated hazard.* Cambridge: Cambridge Uni ersit Press.

Buforn, E., A. Udias and M. A. Colombas. 1988. Seismicit , source mechanisms and tectonics of the Azores-Gibraltar plate boundar . *Tectonophysics*. 152: 89—118.

Caribbean Tsunami Hazard 2006. (Eds. A. Mercado-Irizarr and P.L.-F. Liu). World Sci. Pub., Singapore.

Chen, Q., J. T. Kirb , R. A. Dal ple, A. B. nned , and A. Cha 2000. Boussinesq modeling of a ansformation reaking, and runup. 2-D. *J. Waterway, Port, Coastal and ean Engineer . 126: 48—56.

U.S.G.S. 2001. *Earthquakes and Ts amis in Puert Rico and the U.S. Vir Islands*. USGS Fact Sheet FS-141-00.

Da , S. J., P. Watts, S. T. Grilli, an T. Kirb . 20 . Mechanical Models the 1975 Kalapana, Ha aii Earthquake d Tsunami. M rine Geolog . 215(1-2) 59-92.

DeMets, C. 1993. Earthquake slip ors and estima es of present-da plate otions. *J. Geophys. Res.* 98: 6703—671

Dolan, J. F., and Wald, D. J. 1998. e 1943-1953 rth-central Caribbean thquakes: Acti e tectonic setting, seism hazards, and implications for Carib ean-North America plate motions. *Ge logical Society of America Special P blications*. 326: 143—170.

Driscoll, N. W., J. K.Weissel, and J. A. Goff. 2000. Potential for large-scale submarine slope failure and tsunami gen ration along th U.S. mid-Atlantic coa . *Geology*. 28(5): 407–410.

Dunbar, P. K. and C. S. Wea er. 2 08. U.S. States and Territories Nation l Tsunami Hazard Assessment: Historic Record and Sources for Wa es. Prep red for the National Tsunami Hazard Mit gation Program b *NOAA* and *USGS*.

Enet, F, Grilli, S.T. and P. Watts, 20 3. Laborator E periments for Tsunamis Generated b Under ater Landslides: C mparison ith Numerical Modeling. In *Proc. 13th Offshore and Polar Engng. Conf.* (ISOPE03, Honolulu, USA, Ma 2003), 372-379.

Enet F. and S.T. Grilli 2005. Tsunami Landslide Generation: Modelling and E periments. In *Proc. 5th Intl. on Ocean Wave Measurement and Analysis* (WAVES 2005, Madrid, Spain, Jul 2005), IAHR Publication, paper 88, 10 pps.

Enet, F. and S. T. Grilli. 2007. E perimental stud of tsunami generation b three-dimensional rigid under ater landslides. *J. Waterway, Port, Coastal and Ocean Engineering.*. 133: 442—454.

Fabre, R., E. Tric, J. Riss, T. Lebourg, and S. Abadie. Ne in estigation of potential collapse of the Cumbre Vieja's olcanic ediface (La Palma Island; Spain); numerical e aluation of failure and estimated olume. In re ision.

Fine, I.V., A.B. Rabino ich, B.D. Bornhold, R. E. Thomson, and E.A. Kuliko . 2005. The Grand Banks landslide-generated tsunami of No ember 18, 1929: Prelaminar anal sis and numerical modeling. *Marine Geology*. 215: 45-57.

Fr er, G. L., P. Watts, and L. F. Pratson. 2004. Source of the great tsunami of 1 April 1946: A landslide in the upper Aleutian forearc. *Marine Geology.* 203: 201-218.

Gica, E., M. C. Spillane, V. V. Tito , C. D. Chamberlin, and J. C. Ne man. 2008. De elopment of the forecast propagation database for NOAA's Short-Term Inundation Forecast for Tsunamis (SIFT). NOAA Tech. Memo. OAR PMEL-139.

Geist, E. L., P. J. L[illegible] J. D. Cha tor. 2009. H[illegible]namic Modeling of Tsunamis from the Cu[illegible]andslide. *Marine Geolog*[illegible]: 41-52.

Gisler G., Wea er [illegible]ngs M.L., 2006. Sage cal[illegible]ons of the tsunami threat from La Palma. S[illegible]*f Tsunami Hazard*, 24(4): [illegible]301.

Gracia, E., J. Dañob[illegible] Vergés, and PARSIFAL [illegible]. 2003. Mapping acti e faults offshore Por[illegible]6 degrees N – 38 degrees [illegible] implications for seismic hazard assessment a[illegible]e South est Iberian margi[illegible]*eology*. 32: 83—86.

Grandin, R., J. F. [illegible]s, M. Bezzeghoud, B. [illegible]eira, and F. Carrilho. 2007. Simulations [illegible]ng ground motion in SW[illegible]eria for the 1969 Februar 28 (Ms=8.0) an[illegible]755 No ember 1 (M~ 8.5[illegible]rthquakes – I. Velocit model. II. Strong [illegible]d motion simulations. [illegible]*physical Journal International*. 171(2): 807-[illegible]

Greene, H. G., Mu[illegible] Y., Watts, P., Maher, N. [illegible] Fisher, M. A., Paull, C. E., and Eichhubl, P[illegible]. Submarine landslides [illegible] the Santa Barbara Channel as potential tsu[illegible]ources. *Nat. Hazards and E*[illegible]*h Sci. Systems*. EGU. 6: 63-88.

Grilli, S.T. 1997. F[illegible] Nonlinear Potential Flo M[illegible]els used for Long Wa e Runup Prediction. [illegible]ap[illegible]r in *Long-Wave Runup M*[illegible]*ls,* (eds. H. Yeh, P. Liu, and C. S nolakis), [illegible]s. [illegible]6-180. World Scientific Pu[illegible]shing, Singapore.

Grilli, S. T. and P. [illegible]att[illegible]. 1999. Modeling of a e[illegible]enerated b a mo ing submerged bod . Appl[illegible]cat[illegible]ns to under ater landslide[illegible] *Engng. Anal. Bonud. Elem.* 23: 645—656.

Grilli, S.T., S. Vog[illegible]lma[illegible]n, and P. Watts. 2002. De[illegible]elopment of a 3D numerical a e tank for mo[illegible]deli[illegible]g tsunami generation b un[illegible]er ater landslides. *Engng. Anal. Bound. Ele*[illegible]. 26[illegible] 301—313.

Grilli, S.T. and P[illegible] W[illegible]tts 2001 Modeling of tsun[illegible]mi generation b an under ater landslide in a 3D-NWT. In *Proc. 11th* [illegible]*ffshore and Polar Engng. Conf.* (ISOPE01, Sta [illegible]nger, Nor a , June 2001), V[illegible]l III, 132-139.

Grilli, S. T., and P. Watts. 2005. Tsunami generatio[illegible] b submarine mass failure. Part I: Modeling, e perimental alidation, and sensi[illegible]i it anal sis. *J. Waterway, Port, Coastal and Ocean Engineering.* 131: 283—2[illegible]97.

Grilli, S. T., C. D. P. Ba ter, S. Maretzki, Y. Perignon[illegible], and D. Gemme. 2006. Numerical simulation of tsunami hazard maps for the US East Coast. Tech. rep., FM Global Project.

Grilli, S. T., M. Ioualalen, J.Asa anant, F. Shi, J. Kirb , and P. Watts. 2007. Source Constraints and Model Simulation of the December 26, 2004 Indian Ocean Tsunami. *J. Wtrwy, Port, Coast, and Oc. Engrg.* ASCE. 133(6): 414-428.

Grilli, S. T., S. Dubosq, N. Pophet, C. D. P. Ba ter, and O.-D. S. Ta lor. 2008. Numerical simulation of tsunami runup and flooding on the North Shore of Puerto Rico. Tech. Rep., FMGlobal Project.

Grilli. S.T., O.-D. S. Ta lor, D.P. Ba ter S. Ma etzki. 2009. Probabilistic approach for determining submarine landsli unami azard along the upper East Coast of the United States.Marine Geolog (1-2): 7 -97.

Grilli, S. T., S. Dubosq, N. Pophet, Y érignon, J. T. Kirb , and F. Shi. 2010a. Numerical simulation and first-or azard a al sis of large co-seismic tsunamis generated in the Puerto Rico tre : near-f eld impact on the North shore of Puerto Rico and far-field impact he US East Coast, *Nat. Hazards Earth Syst. Sci.*, 10: 2109–2125.

Grilli, S.T., Dias, F., Gu enne, P., Foch o, C. and F. Enet 2010b. Progress In Full Nonlinear Potential Flo Modeli Of 3D E treme Ocean Wa es. Chapter 3 in *Advances in Numerical Simulatio f Nonlinear Water Waves* (ISBN: 978-981-283-649-6, edited b Q.W. Ma) ol. 11 in Series in Ad ances in Coastal and Ocean Engineering). World Scient c Publishing Co. Pte. Ltd., pps. 75- 128.

Grimison, N. L., and W. Chen. 1986. The Azores-Gibraltar plate boundar : Focal mechanisms, depth of earthquakes nd their tectonical implications. *J. Geophys. Res.* 91: 2029—2047.

Gutscher M. A., M.A. Baptista, J.M. Mir da. 2006.The Gibraltar Arc seismogenic zone (part 2): Constraints on a shallo east dipping fault plane source for the 1755 Lisbon earthquake pro ided b tsunami modeling and seismic intensit . *Tectonophysics*. 426: 153–166.

Hanks, T. C. and H. Kanamori. 1979. A oment magnitude scale. *J. Geophys. Res.* 84: 2348-2350.

Ha ard, N., A. B. Watts, G. K. Wes brook, and J. S. Collier. 1999. A seismic reflection and GLORIA stud of c mpressional deformation in the Gorringe Bank region, eastern North Atlantic. *Ge phys. J. Intl.* 138: 831-850.

Ioualalen, M., B. Pelletier, P. Watts, and M. Regnier. 2006. Numerical modeling of the 26th No ember 1999 Vanuatu tsu ami.*J. Geophys. Res*. 111(C6): 2005JC003249.

Ioualalen, M., J. Asa anant, N. Kae ban ak, S. T. Grilli, J. T. Kirb , and P.Watts, 2007. Modeling the 26 December 2004 Indian Ocean tsunami: Case stud of impact in Thailand. *J. Geophys. Res.* 112: 2006JC003850.

Ioualalen, M., S. Migeon, and O. Sardou . 2010. Landslide tsunami ulnerabilit in the Ligurian Sea: case stud of the 1979 October 16 Nice international airport submarine landslide and of identified geological mass failures, *Geophys. J. Intl.* 181:724–740, doi:10.1111/j.1365-246X.2010.04572.

Johnston, A. 1996. Seismic moment assessment of earthquakes in stable continental regions–III. Ne Madrid 1811-1812, Charleston 1886 and Lisbon 1755. *Geophysical Journal International*. 126: 314—344.

Kenned , A. B., Q. Chen, J. T. Kirb , and R. A. Dalr mple. 2000. Boussinesq modeling of a e transformation, breaking and runup: I. One dimension. *Journal of Waterway, Port, Coastal, and Ocean Engineering*. 126: 39—47.

Kirb , J. T. 2003. Boussinesq models and applications to nearshore a e propagation, surf zone processes and a e-induced currents. In *Advances in Coastal Modeling, and Oceanography.* V. C. Lakhan (Editor). Else ier, Ne York. 67: 1—41.

Kirb , J. T., N. Pophet, F. Shi, and S. T. Grilli. 2009. Basin scale tsunami propagation modeling using Boussinesq models: Parallel implementation in spherical coordinates. In *Proc. WCCE-ECCE-TCCE Joint Conf. on Earthquake and Tsunami*. Istanbul, Turke , June 22-24, 2009.

Knight, B. 2006. Model predictions of Gulf and southern Atlantic coast tsunami impacts from a distribution of sources. *Science of Tsunami Hazards.* 24(5): 304—312.

Lander, J. F., L. S. Whiteside, and P. A. Lockridge, 2002. A Brief Histor of Tsunamis in the Caribbean Sea. *Science of Tsunami Hazards.* 20 (1) 57-94.

Lee, H.J. 2009. Timing occurrence of Large Submarine Landslides on the Atlantic Ocean Margin. Marine Geolog . 264: 53-64.

Locat J., H. Lee, U. S. ten Brink, D T ichell, E. Geist, and M. Sansouc . 2009. Geomorpholog , stabilit and mobilit of the Currituck slide. *Marine Geology*. 264: 28–40.

Lockridge, P. A., L. S. Whiteside, and J. F. Lander. 2002. Tsunamis and tsunami-like a es of the Eastern United States. *Science of Tsunami Hazards*. 20(3): 120—157.

Lø holt, F., G. Pedersen, and G. Gisler. 2008. Oceanic propagation of a potential tsunami from the La Palma Island. *J. Geophys. Res.* 113: C09026, doi:10.1029/2007JC004603.

Mader, C. L., 2001 Modeling the La Palma landslide tsunami. *Science of Tsunami Hazards*. 19: 150-170.

Masson, D. G., A. B. Watts, M. J. R. Gee, R. Urgeles, N. C. Mitchell, T. P. Le Bas, and M. Canals. 2002 Slope failures on the flanks of the estern Canar Islands. *Earth-Science Reviews*. 57: 1—35.

Masson, D. G., C. B. Harbitz, R. B. W nn, G. Pedersen, and F. Lo holt. 2006. Submarine landslides: Processes, triggers, and hazard prediction. *Philosophical Transactions of the Royal Society A*. 264: 2009—2039.

McMurtr , G. M., D. R. Tappin, P. N. Sed ic, I Wilkinson, J. Fietzke, and B. Sell oo. 2007. Ele ated marine deposits in Bermuda record a late Quaternar megatsunami. *Sedimentary Geology.* 200: 155—165.

Mercado, A. and W. McCann. 1998. Numerical Simulation of the 1918 Puerto Rico Tsunami. *Natural Hazards.* 18: 57–76.

Moss, J.L., W.J. McGuire, and D. Page. 1999. Ground deformation monitoring of a potential landslide at La Palma, Canar Islands, *J. Volcanology and Geothermal Research*. 94: 251-265.

Nikolkina I., N. Zahibo and E. Pelino sk . 2010. Tsunami in Guadeloupe (Caribbean Sea). *The Open Oceanography Journal.* 4: 44-49.

Okada, Y. 1985. Surface deformation due to shear and tensile faults in a half-space. *B. Seismol. Soc. Am.* 75(4): 1135—1154.

O'Loughlin, K.F. and Lander, J.F. *Caribbean Tsunamis: A 500-Year History from 1498–1998*. Ad ances in Natural and Technological Hazards Research, V. 20, Klü er, 2003.

Pararas-Cara annis, G. 2002. E aluation of the threat of mega tsunami generation from postulated massi e slope failures of island strato olcanoes on La Palma, Canar Islands, and on the island of Ha aii. *Science of Tsunami Hazards.* 20(5): 251—277.

Perignon, Y. 2006. Tsunami hazard modeling. Tech. rep., Department of Ocean Engineering, Uni ersit of Rhode Island and Ecole Centrale de Nantes.

Pophet, N., 2008. *Parallel computation for tsunami*. M.S. Thesis, Chulalongkorn Uni ersit .

Pophet, N., Ioualalen, M., Asa anant, J., 2010. Parallelization of full nonlinear Boussinesq equations for tsunami simulations: ne approach on higher grid resolution for tsunami simulation using parallelized full nonlinear Boussinesq Equations. *Computers and Fluids…*

Prior, D. B., E. H. Do le, and T. Neurauter. 1986. The Currituck Slide, Mid-Atlantic continental slope; re isited. *Marine Geology*. 73: 25—45.

Rahiman, T. I. H., J. R. Pettinga, and P. Watts. 2007. The source mechanism and numerical modelling of the 1953 Su a tsunami, Fiji. *Marine Geology*. 237(2): 55-70.

Ruffman, A. 2005. Comment on: Tsunamis and Tsunami-like of the Eastern United States b Patricia A. Lockridge, Lo ell S. Whiteside and James Lander ith Respect to The No ember 18, 1929 Earthquake and Its Tsunami. *Science of Tsunami Hazards*. 23(3): 52-59.

S kes, L. R., W. McCann, and A. Kafka. 1982. Motion of Caribbean plate during the last 7 million ears and implications for earlier cenozonic mo ements. *J. Geophys. Res.* 70: 5065—5074.

Tappin, D. R., P. Watts and S. T. Grilli. 2008. The Papua Ne Guinea tsunami of Jul 17, 1998: Anatom of a catastrophic e ent. *Nat. Haz. and Earth Sys. Sci.*, 8: 243-266.

ten Brink, U. S. and J. Lin. 2004. Stress interaction bet een subduction earthquakes and forensic strike-slip faults: Modeling and application to the northern Caribbean plate boundar . *J. Geophys. Res.* 109, B12310.

ten Brink, U. S. 2005. Vertical motions in the Puerto Rico trench and Puerto Rico and their cause. *J. Geophys. Res.* 100: B06404.

ten Brink, U. S., D. T ichell, E. Geist, J. Cha tor, J. Locat, H. Lee, B. Buczko ski, and M. Sansouc 2007. The Current State of Kno ledge Regarding Potential Tsunami Sources Affecting U.S. Atlantic and Gulf Coasts. Report to the Nuclear Regulator Commission. *USGS*. 166 pages.

ten Brink, U. S., D. T ichell, E. Geist, J. Cha tor, J. Locat, H. Lee, B. Buczko ski, R. Barkan, A. Solo , B. Andre s, T. Parsons, P. L nett, J. Lin, and M. Sansouc . 2008. E aluation of Tsunami Sources ith the Potential to Impact the U.S. Atlantic and Gulf Coasts. Report to the Nuclear Regulator Commission. *USGS*. 322 pages.

ten Brink, U. S., H. J. Lee , E. L. Geist, and D. T ichell. 2009a. Assessment of tsunami hazard to the U.S. East Coast using relationships bet een submarine landslides and earthquakes. *Marine Geology*. 264: 65–73.

ten Brink, U.S., R. Barkan, B.D. Andre s, and J.D. Cha tor. 2009b. Size distributions and failure initiation of submarine and subaerial landslides. *Earth and Planetary Science Letters*. 287: 31–42.

T ichell, D. C., J. D. Cha tor, U.S. ten Brink, and B. Buczko ski. 2009, Morpholog of Late Quaternar Submarine Landslides along the U.S. Atlantic Continental Margin. *Marine Geology*. 264: 4-15.

U.S.G.S. April 2001. Earthquakes and Tsunamis in Puerto Rico and the U.S. Virgin Islands. USGS Fact Sheet FS–141–00

Walder, J.S., P. Watts, and C.F. Wa thomas. 2006. Mapping tsunami hazards associated ith debris flo into a reser oir. *J. Hyd. Eng.* ASCE. 132(1): 1-11.

Ward S. N. 2001.Tsunamis. *Encyclopedia of Physical Science and Technology* .175-191,

Ward, S. N. and S. Da . 2001. Cumbre Vieja Volcano – potential collapse and tsunami at La Palma, Canar Islands. *Geophys. Res. Lett.* 21: 397—400.

Watts, P. and Grilli, S.T., 2003. Tsunami Generation b Deformable Under ater Landslides. In *Proc. 13th Offshore and Polar Engng. Conf.* (ISOPE03, Honolulu, USA, Ma 2003), 364-371.

Watts, P., S. T. Grilli, J. T. Kirb , G. J. Fr er, and D. R. Tappin. 2003. Landslide tsunami case studies using a Boussinesq model and a full nonlinear tsunami generation model. *Nat. Hazards Earth Syst. Sci.* 3: 391—402.

Watts, P., S. T. Grilli, D. Tappin, and G. J. Fr er. 2005. Tsunami generation b submarine mass failure. Part II: predicti e equations and case studies. *J. Waterw. Port, Coast. Ocean Engng.* 131: 298—310.

Watts, P. 2006. Case stud of the 1755 Portugal tsunami. Final report for Risk Management Solutions, Inc.

Wa thomas, C. F., P. Watts, and , J. S. Walder. 2006. Numerical simulation of tsunami generation b cold olcanic mass flo s at Augustine olcano, Alaska. *Nat. Haz. And Earth Sys. Sci.* NHESS. 6: 671-685.

Wei, G., and J. T. Kirb . 1995. Time-dependent numerical code for e tended Boussinesq equations. *J. Wtrwy, Port, Coast, and Oc. Engrg.* ASCE. 121(5): 251-261.

Wei, G., J. T. Kirb , S. T. Grilli, and R. Subraman a. 1995. A full nonlinear Boussinesq model for free surface a es. Part 1: Highl nonlinear unstead a es. *J. Fluid Mech.* 294: 71-92.

W nn, R. B. and D. G. Masson. 2003. Canar Island landslides and tsunami generation: can e use turbidite deposits to interpret landslide processes? *In* Locat, J., and J. Meinert (Editors), Submarine mass mo ements and Their Consequences, Klu er, Dordrecht. 325—332.

Zahibo, N. and E. N. Pelino sk . 2001. E aluation of tsunami risk in the Lesser Antilles. *Natural Hazards and Earth System Sciences*. 1: 221–231.

Zahibo, N., E. Pelino sk , A. Yalciner, A. Kurkin, A. Koselko , and A. Zaitse , 2003a. The 1867 Virgin Island Tsunami: obser ations and modeling. *Oceanologica Acta.* 26: 609—621.

Zahibo N., E. Pelino sk , A. Kurkin, and A. Kozelko . 2003b. Estimation of far-field tsunami potential for the Caribbean coast based on numerical simulation. *Science of Tsunami Hazards.* 21 (4): 202-222.